

# **TRANS NOW**

TRANSPORTATION NORTHWEST

**Final Report TNW 2012-11**

**TransNow Contract No.: 699207**

## **ENHANCED PERFORMANCE OF RECYCLED AGGREGATE CONCRETE WITH ATOMIC POLYMER TECHNOLOGY**

Pizhong Qiao, Ph.D., P.E.  
Professor

Fangliang Chen, Ph.D.  
Post-Doctoral Research Associate

**Washington State Transportation Center (TRAC)**

Washington State University  
Department of Civil & Environmental Engineering  
Pullman, WA 99164-2910

A report prepared for

**Transportation Northwest (TransNow)**  
University of Washington  
129 More Hall Box, UW Box 352700  
Seattle, WA 98195-2700

in cooperation with

**U.S. Department of Transportation**  
Federal Highway Administration

June 2012

**TECHNICAL REPORT STANDARD TITLE PAGE**

1. REPORT NO. TNW2012-11	2. GOVERNMENT ACCESSION NO.	3. RECIPIENT'S CATALOG NO.	
4. TITLE AND SUBTITLE ENHANCED PERFORMANCE OF RECYCLED AGGREGATE CONCRETE WITH ATOMIC POLYMER TECHNOLOGY		5. REPORT DATE 6/2012	
		6. PERFORMING ORGANIZATION CODE 62-0948	
7. AUTHOR(S) Pizhong Qiao, Fangliang Chen, Ph.D		8. PERFORMING ORGANIZATION REPORT NO. TNW2012-11	
9. PERFORMING ORGANIZATION NAME AND ADDRESS Transportation Northwest Regional Center X (TransNow) Box 352700, 112 More Hall University of Washington Seattle, WA 98195-2700		10. WORK UNIT NO.	
		11. CONTRACT OR GRANT NO. DTRT07-G-0010	
12. SPONSORING AGENCY NAME AND ADDRESS United States Department of Transportation Office of the Secretary of Transportation 1200 New Jersey Ave, SE Washington, D.C. 20590		13. TYPE OF REPORT AND PERIOD COVERED Final Technical Report	
		14. SPONSORING AGENCY CODE	
<p>ABSTRACT</p> <p>The atomic polymer technology in form of mesoporous inorganic polymer (MIP) can effectively improve material durability and performance of concrete by dramatically increase inter/intragranular bond strength of concrete at nano-scale. The strategy of MIP is fundamentally different from most additives currently on the market for industrial applications. When MIP is added to a concrete or masonry mix, this atomic-level bonding means that the strength of the cement is defined by the strength of its atomic bonds; these bonds are incredibly strong. Atomic-level bonding also translates the flexibility of the MIP molecule, which is built like a coil, lending strong tensile and flexural strength, thus reducing the vulnerability of concrete to cracking. On the other hand, the recycle concrete aggregates from the demolished structures, when reused in concrete, often exhibit relatively low mechanical performance. It is thus anticipated that the inclusion of MIP in recycle aggregate concrete (RAC) can effectively improve its performance and long term durability. The objectives of the proposed study are two-fold: (1) to evaluate the performance of RAC with MIP, and (2) to assess improved performance and condition of RAC using embedded smart piezoelectric sensors/actuators. The findings in RAC with MIP resulted from this study will promote the widespread application of recycled concrete in engineering, improve sustainability of RAC structures, and provide viable long term health monitoring techniques for RAC.</p>			
17. KEY WORDS Recycled aggregate concrete		18. DISTRIBUTION STATEMENT No restrictions.	
19. SECURITY CLASSIF. (of this report) None	20. SECURITY CLASSIF. (of this page) None	21. NO. OF PAGES 79	22. PRICE

## **DISCLAIMER**

The contents of this report reflect the views of the authors, who are responsible for the facts and the accuracy of the information presented herein. This document is disseminated under the sponsorship of the Department of Transportation University Transportation Centers Program, in the interest of information exchange. The U.S. Government assumes no liability for the contents or use thereof.

## Table of Contents

	Pages
<b>LIST OF TABLES.....</b>	<b>VII</b>
<b>LIST OF FIGURES .....</b>	<b>VIII</b>
<b>CHAPTER 1 INTRODUCTION.....</b>	<b>1</b>
1.1 PROBLEM STATEMENT.....	2
1.2 RESEARCH BACKGROUND.....	4
1.3 RESEARCH OBJECTIVES .....	4
<b>CHAPTER 2 LITERATURE REVIEW .....</b>	<b>6</b>
2.1 RECYCLED AGGREGATE SOURCES.....	6
2.2 PROPERTIES OF RA AND RAC .....	7
2.2.1 Properties of recycled aggregate.....	7
2.2.2 Properties of recycled aggregate concrete .....	8
2.2.2.1 Compressive strength.....	9
2.2.2.2 Modulus of elasticity.....	11
2.2.2.3 Flexural and splitting tensile strength.....	12
2.2.3 Durability of recycled aggregate concrete .....	13
2.2.4 Shrinkage and creep.....	15
2.2.4.1 Plastic shrinkage .....	15
2.2.4.2 Autogenous shrinkage.....	15
2.2.4.3 Drying shrinkage.....	16
2.2.4.4 Test methods of concrete shrinkage .....	16
2.2.4.5 Shrinkage test results in the literature .....	18
2.3 HEALTH MONITORING OF CONCRETE USING PIEZOELECTRIC MATERIALS .....	19
2.4 ENHANCED PERFORMANCE OF RAC WITH DIFFERENT ADMIXTURES.....	21
2.4.1 Atomic polymer technology (APT) .....	22

2.4.2	Enhancing mechanism of concrete with APT .....	22
2.4.2.1	Increased compression and tensile strength .....	22
2.4.2.2	Increased durability .....	23
<b>CHAPTER 3 TEST PROGRAMS FOR RECYCLED AGGREGATE CONCRETE</b>		
.....		<b>25</b>
3.1	FREE SHRINKAGE TEST .....	25
3.2	RESTRAINED FREE SHRINKAGE TEST .....	25
3.3	DYNAMIC MODULUS TEST .....	27
3.4	ELASTIC WAVE-BASED METHOD .....	32
<b>CHAPTER 4 MATERIALS AND SAMPLE FABRICATION.....</b>		<b>35</b>
4.1	MATERIALS AND MIX DESIGN .....	35
4.1.1	Aggregates .....	35
4.1.2	Chemical admixtures .....	37
4.1.3	Mix designs .....	38
4.2	SMART AGGREGATES FABRICATION.....	39
4.3	CONCRETE MIXING AND SAMPLE PREPARATION .....	41
4.3.1	Concrete beam samples with embedded smart aggregates .....	41
4.3.2	Concrete ring samples .....	42
<b>CHAPTER 5 TEST RESULTS AND ANALYSIS .....</b>		<b>45</b>
5.1	TEST RESULTS FOR FRESH CONCRETE.....	45
5.2	TEST RESULTS FOR HARDENED CONCRETE .....	46
5.3	DYNAMIC MODULUS TEST RESULTS .....	48
5.4	MODULUS OF ELASTICITY BASED ON WAVE TEST RESULTS .....	50
5.5	COMPARISONS OF MODULUS OF ELASTICITY AMONG DIFFERENT TEST METHODS	
	.....	52
5.6	SHRINKAGE TEST RESULTS .....	53

5.6.1	Free shrinkage test results.....	53
5.6.2	Restrained shrinkage test results.....	57
<b>CHAPTER 6</b>	<b>CONCLUSIONS AND RECOMMENDATIONS .....</b>	<b>61</b>
6.1	CONCLUSIONS.....	61
6.2	RECOMMENDATIONS .....	63
<b>ACKNOWLEDGEMENTS .....</b>		<b>64</b>
<b>REFERENCES .....</b>		<b>65</b>

## List of Tables

	Pages
Table 2.1 Physical and mechanical properties of two kinds of aggregates (Adom-Asamoah et al., 2010).....	9
Table 4.1 Coarse Recycled Aggregate Gradations (Sieve Analysis) .....	36
Table 4.2 Specific Gravity and Water Absorption of the 1-1/4” Recycled Aggregates ....	36
Table 4.3 Fine Aggregate Gradation (Sieve Analysis).....	37
Table 4.4 Rational Chemical Admixture Range.....	38
Table 4.5 WSDOT Mix #0948 with and without APT.....	39
Table 4.6 Chemical Admixtures in Different Batches .....	39
Table 5.1 Material Properties of Fresh Concrete .....	46
Table 5.2 Material Properties of Hardened Concrete.....	48
Table 5.3 Modulus of Elasticity by Different Methods at 7 and 28 days .....	53
Table 5.4 Free Shrinkage Test Data (in microstrain) .....	56
Table 5.5 Restrained Ring Test Data (days of cracking).....	57

## List of Figures

	Pages
Figure 1.1 Composition of Concrete.....	1
Figure 1.2 Consumption of Natural Aggregate in the United States (Kelly, 1998). .....	2
Figure 2.1 Recycled Aggregates (RA). .....	7
Figure 2.2 Stress-strain Diagram of NAC and RAC (Xiao et al., 2005). .....	12
Figure 3.1 Diagrams of Ring Specimen Used (Reprinted from AASHTO PP34-99).....	27
Figure 3.2 Time Domain Impulse Signal. ....	29
Figure 3.3 Time Domain Response Data. ....	29
Figure 3.4 Frequency Domain Response Data. ....	30
Figure 3.5 Setup for Dynamic Modulus Test. ....	31
Figure 3.6 Experimental Setup for Health Monitoring of RAC Prism in Smart Structures Lab at WSU.....	33
Figure 3.7 Input and Output Signals Captured by Smart Aggregate. ....	33
Figure 4.1 Recycled Aggregates. ....	35
Figure 4.2 Fabrication Process of Smart Aggregate. ....	40
Figure 4.3 Schematic of Fabrication Process of Smart Aggregate. ....	40
Figure 4.4 Plastic Mold for Fabrication of Smart Aggregate Concrete Mixing and Sample Preparations.....	40
Figure 4.5 Isolation of Smart Aggregates with Electric Tapes. ....	41
Figure 4.6 Concrete Beam Specimen and Placement of Embedded Smart Aggregates. ..	42
Figure 4.7 Restrained Shrinkage Ring Apparatus. ....	43

Figure 4.8. Top Surface Sealing of the Ring Samples. ....	44
Figure 4.10 Ring Test Setup in the Condition Room. ....	44
Figure 5.1 Slump Test of Fresh RAC. ....	45
Figure 5.2 Air Content Test. ....	46
Figure 5.3 Compressive and Modulus of Elasticity Test. ....	47
Figure 5.4 Flexural Strength Test. ....	48
Figure 5.5 Variance of Frequency with Respect to Curing Time. ....	49
Figure 5.6 Variance of Dynamic MOE with Respect to Curing Time. ....	50
Figure 5.7 Variance of $E_w$ with Respect to Curing Time. ....	51
Figure 5.8 Variance of $G_w$ with Respect to Curing Time. ....	52
Figure 5.9 Free Shrinkage Test Setup. ....	54
Figure 5.10 Free Shrinkage of RAC with Different Amount of APT. ....	56
Figure 5.11 Restrained Shrinkage of Ring Specimen without APT. ....	58
Figure 5.12 Restrained Shrinkage of Ring Specimen with 3 oz APT/gallon of Water. ....	59
Figure 5.13. Restrained Shrinkage of Ring Specimen with 5 oz APT/gallon of Water. ....	60

## Chapter 1 Introduction

Concrete is one of the most extensively used construction materials in the world due to its versatility, durability, and economy. The U.S. uses about 180 million cubic meters (240 million cubic yards) of ready-mixed concrete each year. It is used in highways, streets, parking lots, parking garages, bridges, high-rise buildings, dams, homes, floors, sidewalks, driveways, and numerous other applications. Concrete is a mixture of cement (or a combination of cementitious materials), fine aggregate (sand), coarse aggregate (gravel or crushed stone), and water. Coarse aggregate amounts to about 41% in the bulk of concrete (**Figure 1.1**). Obviously, production of concrete will not only consume a large quantity of energy but also a considerable amount of stone or rock resources.

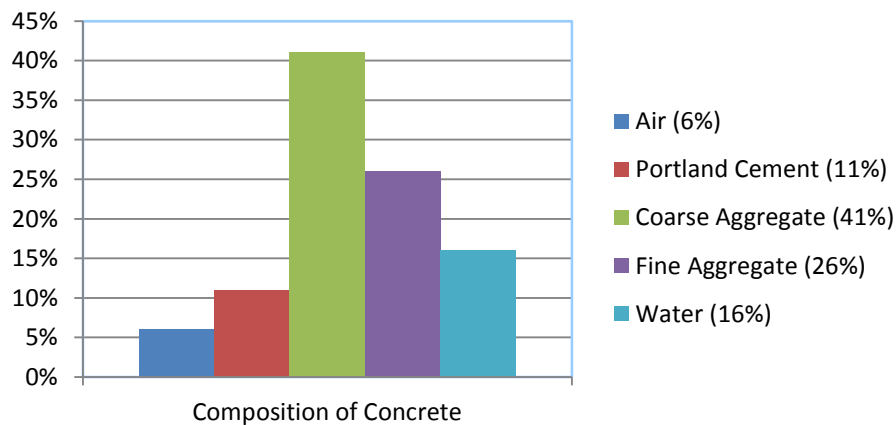


**Figure 1.1 Composition of Concrete.**

The changes of consumption of natural aggregate in the United States back to the earlier of last century are shown in **Figure 1.2**. The use of natural aggregates (includes crushed stone, sand and gravel) had grown significantly from 500 million metric tons in 1900 to 27,800 million metric tons in 1998. According to the report by United State

Geological Survey (USGS), based on the assumptions of an average annual growth rate of 0.1% for the production of crushed stone and 0.5% for sand and gravel, the consumption of natural aggregates is expected to increase to 2.7 billion metric tons (Kelly, 1998). Under this circumstance, the USGS's report also highlights that some areas may lack of quality aggregates, or existing aggregates deposits cannot be mined for a multitude of reasons. Moreover, the ecological environment would be impacted adversely by consuming such a great deal of aggregates as well as by producing cement which also takes a fair amount in the concrete. Statistics indicate that the carbon emissions from cement industry make up about 7% of total emissions.

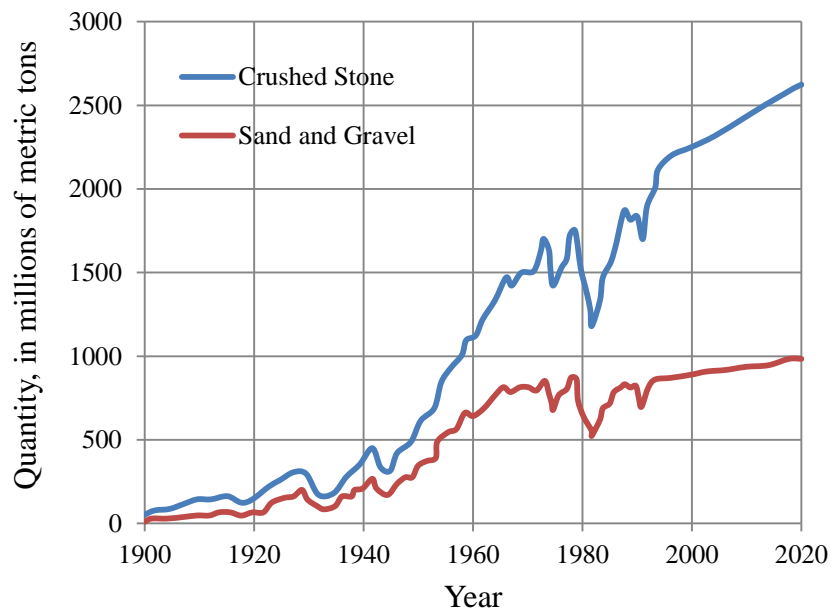


**Figure 1.2 Consumption of Natural Aggregate in the United States (Kelly, 1998).**

### 1.1 Problem Statement

The waste concrete resulting from construction and demolition work in the United States constitutes about 29% of solid waste (Rogoff and Williams, 1994). As a sort of waste produced by demolishing old buildings, concrete waste results in serious

environment pollution and vast resource extravagance if it is not reutilized or recycled. From the viewpoints of going green (i.e., environmental preservation and effective utilization of resources), reducing the carbon footprint, and increasing the sustainability and growth of transportation systems, it is beneficial and imperative to reuse waste concrete as recycled aggregates (RA) for new construction. Recycling concrete wastes, especially from the demolished transportation and building structures, will lead to reduction in valuable landfill space and savings in natural resources. There is also a growing need to utilize recycled aggregates to replace natural aggregates as good quality gravel sources are increasingly becoming exhausted.

Concrete recycling gains importance because it protects natural resources and eliminates the need for disposal by using the readily available concrete as an aggregate source for new concrete or other applications. In the last two decades, the recycling of demolished concrete wastes for Recycled Aggregate (RA) has already been proven to be a commercial and feasible way applied in the field of construction, especially for those non-structural applications. According to a 2004 FHWA study (<http://www.fhwa.dot.gov/pavement/recycling/rca.cfm>), 38 states recycle concrete as an aggregate base; 11 states recycle it into new Portland cement concrete. Such recycling techniques can effectively lower the consumption of limited landfill, while reducing considerable manufacture and transport costs. The use of recycled aggregate concrete (RAC) acquires particular interest in transportation infrastructure regarding its sustainable development. Usually, recycled aggregates have greater porosity and water absorption, lower density, and lower strength than natural aggregates, and the recycle concrete aggregates from the demolished structures, when reused in concrete, often exhibit relatively low mechanical performance. However, very limited research has been explored on performance enhancing of recycled aggregate concrete.

## **1.2 Research Background**

The atomic polymer technology (APT) in form of mesoporous inorganic polymer (MIP) can effectively improve material durability and performance of concrete by dramatically increasing inter/intragranular bond strength of concrete at nano-scale. The strategy of MIP is fundamentally different from most additives currently on the market for industrial applications. When MIP is added to a concrete or masonry mix, this atomic-level bonding means that the strength of the cement is defined by the strength of its atomic bonds; these bonds are incredibly strong. Atomic-level bonding also translates the flexibility of the MIP molecule, which is built like a coil, lending strong tensile and flexural strength, thus reducing the vulnerability of concrete to cracking. Other characteristics of MIP like fireproofing, self-deicing, antimicrobial features and VOC sequestration are also added. A preliminary study conducted by the PI showed that about 27% in stiffness and 45% in compressive strength were increased for the concrete with MIP. It is thus anticipated that the inclusion of MIP in recycle aggregate concrete (RAC) can effectively improve its performance and long term durability.

On the other hand, with advancement of sensor and wireless communication technologies, it is now becoming more viable to monitor and assess condition of transportation structures, particularly being built with RAC. The embedded piezoelectric sensors and actuators in the RAC structures should be capable of monitoring the properties and conditions (including damage), especially the long term performance, of the RAC structures, contributing to smart infrastructure initiatives. However, the potential and validity of smart materials for effective damage detection and health monitoring of concrete structures have not been fully explored.

## **1.3 Research Objectives**

To better evaluate the early as well as long term performance and conditions of

structures made of recycled aggregate concrete (RAC) with atomic polymer technology (APT) and monitor the early stiffness gaining process with smart piezoelectric material, the objectives of this study will be addressed through the completion of the following two major tasks:

1. To evaluate the performance, in particular of the early free and restrained shrinkage behavior of RAC with APT;
2. To assess improved performance and condition of RAC with APT using embedded smart piezoelectric sensors/actuators; and
3. To reach conclusions and develop recommendations to set the stage for further long-term evaluation.

A combined experimental and theoretical approach will be conducted to develop the condition assessment and degradation detection strategy using smart materials and evaluate the performance enhancement of RAC structures with APT. The findings in RAC with APT resulted from this study will potentially promote the widespread application of recycled concrete in engineering, improve sustainability of RAC structures, and provide viable long term health monitoring techniques for RAC structures.

## **Chapter 2 Literature Review**

Waste concrete accounts for a great proportion (approximately 40%) of the demolition wastes (Oikonomou, 2005). The waste concrete caused by demolishing or originated from construction industry in the United States constitutes about 29% of solid waste (Rogoff and Williams, 1994). It will cost not only tremendous of money to dispose these waste but also precious land resources used as landfills, and more adversely, the local environment will be polluted inevitably. To save environmental and cost, the waste resulting from the demolished construction can be recycled and reused in new construction projects. The so-called Recycled Aggregate Concrete (RAC) can be explained as concrete being produced by using crushed waste concrete as its total or partial aggregate.

The use of crushed waste concrete as aggregate for producing new concrete began in Europe at the end of World War II. It was primarily applied in pavement constructions. In recent years, the RAC technology has been developed rapidly. In the United States, more than 20 states have used RAC in civil infrastructure. It is anticipated that RAC will be increasingly used in many years to come, because increasing reuse of waste concrete offers an effective green solution (i.e., environmental preservation and effective utilization of resources), reduces the carbon footprint, and increases the sustainability and growth of transportation systems.

### **2.1 Recycled Aggregate Sources**

Recycling of concrete is a relatively simple process. It involves breaking, removing, and crushing existing concrete into a material with a specified size and quality. Thus, the quality of concrete with RCA is very dependent on the quality of the recycled material used. Recycled concrete aggregates contain not only the original aggregates, but also

hydrated cement paste. This paste reduces the specific gravity and increases the porosity compared to similar virgin aggregates. Higher porosity of RCA leads to a higher absorption.

## 2.2 Properties of RA and RAC

### 2.2.1 Properties of recycled aggregate

The shapes of recycled aggregates (RA) are similar to those of natural aggregates (NA); but the appearances of RA tend to be more angular and rougher, as shown in **Figure 2.1**. The crushing of virgin aggregate particles and the mortar adhered to the surfaces of virgin aggregate are the major causes for more angular and rougher shapes. In addition, the crushing process can lead to numerous micro-cracks in the RA. Generally, RA has a higher water absorption capacity and lower gravity compared to NA.



**Figure 2.1 Recycled Aggregates (RA).**

Hansen and Narud (1983) reported that the special gravity of RA is lower than that of NA. According to their experimental data, the specific gravities of RA with the diameters of 4-8 mm and 16-32 mm are 2,340 and 2,490 kg/m<sup>3</sup>, respectively; while the specific gravities of NA for the same diameter ranges are 2,500 and 2,610 kg/m<sup>3</sup>, respectively. They also pointed out that RA has higher water absorption capacity. The absorption ratio

of RA is about 8.7% for the diameter of 4 to 8 mm and 3.7% for the diameter of 16 to 32 mm, which are many times higher than NA's. The higher water absorption ratio of RA was also observed by several other studies (Building Contractors Society of Japan (BCSJ), 1978; Nixon, 1978; Hasaba et al., 1981; Kreijger, 1983). Topcu and Sengel (2004) further explained that the major causes of high water absorption capacity of RA are due to mortar (old cementitious paste) in RA and lower density of RA.

Although beneficial progress has been gained over the last decade by applying RA into construction materials in the form of RAC members, there are still many problems concerning how to determine some basic engineering properties properly and to classify them into practice for convenience. Dhir and Paine (2007) described an experimental project to detect the possibility of using an alternative method for grading recycled aggregates that would overcome the current barriers and concerns with recycled aggregate that restricts their specification and use in concrete. Nataraja and Das (2011) carried out some new re-proportioned mixes for varied compressive strength, and they provided some suggestions to stepwise promote the qualities of RA regarding to its low strength. Adom-Asamoah and Afrifa (2010) investigated the concrete physical and mechanical properties with phyllite coarse aggregates by testing a set of five mixed concrete members with various mixture and acquiring series of typical experimental codes of water absorption, specific gravity, dry density, aggregate impact value, aggregate crushing value, elongation index and Los Angeles abrasion values satisfying the minimum requirement for coarse aggregates suitable for concrete mass production (as shown in **Table 2.1**).

### **2.2.2 Properties of recycled aggregate concrete**

Traditionally, concrete is considered as a three-phase material composed of aggregate, cementitious paste and the interfacial transition zone (ITZ) between coarse aggregate and cement paste. It is well known that with normal concrete mixtures the ITZ has a

significant effect on the strength of concrete (Nilsen and Monteiro, 1993). But for RAC, it is more complex because the ITZs of NA-cement and RA-cement are both present in RAC. Though there are many factors contributing to the relatively poor mechanical properties of RAC, it is widely recognized that the co-existed ITZs in RAC are one of the main reasons.

**Table 2.1 Physical and mechanical properties of two kinds of aggregates (Adom-Asamoah et al., 2010)**

Physical property	Phyllite aggregates	Granite aggregates
Specific gravity	2.72	2.64
Water absorption (%)	1.80	2.30
Aggregate impact (%)	9.80	10.50
Aggregate crushing (%)	18.64	16.42
Ten (%) fines (kN)	255.75	278.45
Flakiness index (%)	28.00	15.00
Elongation index (%)	25.00	2.00
Los Angeles abrasion	17.50	16.25

### **2.2.2.1 Compressive strength**

Some studies reported that RAC has a higher compressive strength than NAC. Yoda and Yoshikane (1988) and Ridzuan et al. (2001) concluded that RAC has a higher compressive strength which is 8.5% and 2 to 20% higher than that of natural aggregate concrete (NAC) in their respective experiments. But, most tests showed a decline in the compressive strength of RAC when compared to NAC. Frondistou-Yannas (1977) evaluated the compressive strength of RAC cylinders and found that it is 4 to 14% lower than that of NAC of the same compositions. Ravindrarajah and Tam (1985) also found a reduction in compressive strength of up to 25% of RAC in comparison to that of NAC.

Others considered that the difference of compressive strength between RAC and NAC is very slight, and the compressive strength of RAC is closely related to the properties of waste concrete. Hansen and Narud (1983) studied the compressive strength of RAC as a function of the compressive strength of waste concrete, and they

concluded that the compressive strength of RAC is fairly affected by the water-cement ratio of the waste concrete when other factors are essentially identical. Tavakoli and Soroushian (1996) used two sources of crushed concrete pavements from two projects in Michigan as aggregates in their experiment. All the fine aggregates in the RAC and NAC mixtures were 100% natural sands. The test results indicated that RAC with a higher compressive strength could be resulted if the compressive strength of the waste concrete was higher than that of the control concrete. Limbachiya et al. (2000) used RA to fabricate high strength concrete (7,252 psi (50 N/mm<sup>2</sup>) or higher). The standard strength testing was carried out at ages 7, 28, 60 and 90 days, and the test results showed that the strength developments with respect to ages for RAC and NAC are similar and RAC with the replacement ratio of coarse RA below 30% has no effect on the strength of concrete, followed by the reduced strength with increasing replacement ratio of RA over 30%.

Generally, use of RA in concrete led to lower cube strength after 28 days than the usage of the equivalent natural aggregate concrete. Dhir and Paine (2007) suggested that it is necessary to reduce the w/c ratio in RAC to achieve equal cube strength with NAC. An important requirement for use of RA in concrete is that it does not lead to significant changes in the w/c ratio. Rao et al. (2011)'s study also illustrated that the strength gain rate for RAC is slower than concrete with natural aggregates in the first 28 days. Liu and Xiao (2011)'s study indicated that new hardened mortar has more significant influences on both the strength and Young's modulus of RAC, when compared with old hardened mortar. Du, et al. (2010)'s test results showed that the peak stress, peak strain, secant modulus of the peak point and original point increase with the strength grade of RA enhanced, whereas the residual stress of RAC decreases with the strength grade enhancing. Fonseca, et al. (2011) studied the relationship between the compressive strength of RAC and the displacement ratios of RA with different specified age and

different curing conditions, and the results revealed that the compressive strength of RAC is not affected obviously by adding more proportions of RA under certain specified curing conditions compared with the normal aggregate concrete members.

In summary, the compressive strength of RAC will be affected by the quality of recycled aggregates. If the w/c ratio is kept constant and the loss of workability due to the effect of using recycled aggregate is compensated for with additives, the percentage of replacement of the recycled aggregate will not significantly affect the compressive strength. The reduction in the compressive strength of RAC can be attributed to the following factors: (1) relatively high porosity of RAC, (2) the weakened areas in the interfacial transition zones (ITZs) of RAC, and (3) lower strength of RA. The contradictory conclusions on the compressive strength with RAC may be due to the differences in the strength of waste concrete, crushing techniques as well as the test methods of experiments considered by different researchers.

#### **2.2.2.2 Modulus of elasticity**

Frondistou-Yannas (1977) reported a significant difference (up to 40% lower in RAC) in the modulus of elasticity (MOE) between RAC and NAC and attributed the lower MOE in RAC as a result of lower MOE of RA. Ravindrarajah et al. (1985) reported that the reduction in the MOE of RAC could be up to 30% when compared to NAC. Hansen and Boegh (1985) evaluated both the static and dynamic moduli of RAC and NAC. Both the static and dynamic moduli reduce about 11% to 28% for RAC, and the reduced elastic modulus even reach 50% when the low strength recycled aggregates were used to produce RAC. López-Gayarre et al. (2009) evaluated the influence of quality and the replacement ratio of RA on the MOE of RAC, and they found that the quality of RA is the only influential factor for the MOE of RAC when the replacement ratio of RA does not exceed 50%.

Xiao et al. (2005) investigated the stress-strain relationships of RAC with different

replacement ratios of RA (**Figure 2.2**). In their study, a comprehensive analysis was performed to evaluate the elastic modulus and the peak and ultimate strains of RAC. They found that the replacement ratio of RA does not have a considerable influence on the stress–strain curves of RAC (**Figure 2.2**).

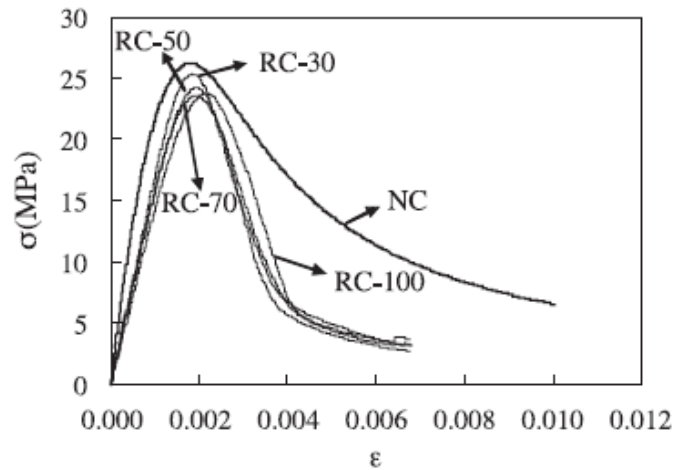


**Figure 2.2 Stress-strain Diagram of NAC and RAC (Xiao et al., 2005).**

The dynamic and static moduli of elasticity of recycled aggregates concrete tested in dry state (Jankovic et al., 2010) indicated that the dynamic modulus of elasticity of RAC members are generally greater than the static modulus of elasticity on the same strength level concrete. The comparison of their testing results also presented that the modulus of elasticity of concrete members are obviously various with the different influence factors of the conditions of manufacture, moisture content, testing equipments and methods.

### **2.2.2.3 Flexural and splitting tensile strength**

Building Contractors Society of Japan (BCSJ, 1978) studied the relationship between the flexural strength and compressive strength of RAC and found that the flexural strength is about 1/8 to 1/10 of the compressive strength. Ravindrarajah and Tam (1985) also showed that the flexural strength of RAC is relatively lower, which is about a 10% decrease in comparison with NAC. Salem (1996) applied the empirical equations of

different mechanical properties (e.g., the tensile and flexural strength vs. the compression strength) for NAC supplied by the ACI code to RAC and evaluated their suitability for RAC. The study found that the conversion function between the tensile and compressive strength was compatible for RAC, but the conversion function between the flexural and compressive strength was conservative. Brito et al. (2004) used three prismatic specimens of  $1.97 \times 15.75 \times 23.62$  in. ( $50 \times 400 \times 600$  mm) to assess the flexural strength of RAC and reported that the flexural strength decreases when the replacement percentage of limestone aggregates with ceramic aggregates increases. Ajdukiewicz and Kliszczewicz (2002) evaluated the splitting strength of RAC based on the pullout method recommended by RILEM and reported that the average decrease of splitting strength is about 20% for the concrete with fully recycled aggregates.

### **2.2.3 Durability of recycled aggregate concrete**

Debieb et al. (2010) conducted a comprehensive study on the mechanical and durability properties of RA concrete members, and it showed that the common degradation of concrete structures due to chlorides and sulphates penetration can be strongly affected by the porosity and the high water absorption of RA. Due to the greater porosity of the recycled aggregate, the elastic modulus of the elaborated recycled concretes diminishes as the replacement ratio increases (Domingo, et al., 2010).

Ryu (2002) performed the chloride penetration test to examine the chloride ion permeability of RA. The RAC prisms were made of three types of RA and two water-cement ratios (i.e., 25% and 55%). Test results indicated that the depth of chloride ion penetration in RAC was larger than that of NAC. The mean value of chloride ion penetration depths of all the RAC reached 10.8 mm when the water-cement ratio was 0.55; whereas the mean value of chloride ion penetration depths of NAC was about 9.7 mm.

Buyle-Bodin and Hadjieva-Zaharieva (2002) compared the durability behaviors of

RAC and NAC, such as the water absorption, air permeability, and carbonation. Two kinds of RAC were considered: one used sand as its fine aggregate, while the other used fine RA. The influence of curing conditions was discussed. The test results showed that RAC has nearly 4 times higher of initial absorption, air permeability, and the carbonation rate. When both the fine and coarse RAs were used in the RAC mix, the permeability is about 6.5 times higher than that of RAC with the sand as its fine aggregate and 13 times higher than that of NAC. The results indicated that the curing conditions also have a significant effect on air permeability of RAC, and the air permeability of RAC cured in air increases about 3 times than that cured in water.

Levy and Helene (2004) analyzed the durability of RAC and concluded that when the NA is replaced by 20% of the RA, RAC is likely to perform the same as the reference concrete made of NA in terms of water absorption, total pore volume, and carbonation. However, the water absorption increases when the amount of NA is replaced by RA of more than 20% because the fine and coarse RAs have 6–10 times higher of water absorption rate than that of NA.

Salem et al. (2003) used the relative dynamic modulus of elasticity to assess the resistance of RAC to freezing and thawing (F/T), and their test showed that the use of RA in the replacement of NA reduces the freezing and thawing resistance of concrete due to the relatively high water absorption of RAC. For NAC, adjusting the water-to-cement (w/c) ratio can improve its resistance to freezing and thawing; while it is not so effective for RAC. The use of proper air entraining can significantly enhance the resistance of RAC to freezing and thawing. Zaharieva et al. (2004) studied the frost resistance of RAC, and they found that when the relative length change of RAC reached 500 m/m, both the compressive and splitting tensile strengths decrease by 10% to 20%; while after 300 F/T cycles, the strengths of RAC are practically exhausted, but the strengths of NAC are usually unchanged even after 300 F/T cycles.

## **2.2.4 Shrinkage and creep**

The shrinkage phenomenon is crucial in some special RAC members, which affects both the short and long term behaviour of this type of concrete. Generally, there are three different kinds of shrinkage for concrete: plastic shrinkage, autogenous shrinkage and drying shrinkage. Plastic shrinkage and autogenous shrinkage happen at an early age of the concrete, while drying shrinkage takes place over a long period of time.

### **2.2.4.1 Plastic shrinkage**

Plastic shrinkage is caused by a rapid loss of water on the concrete surface before the concrete hardens. This loss of water can be caused by many reasons, such as evaporation or suction by a dry sub-base. In the fresh concrete, concrete materials have not formed into a whole body and are still surrounded by water. When too much water rapidly evaporates, the water that remains in the concrete will not be sufficient, and voids occur within concrete, leading to the occurrence of plastic shrinkage cracking. According to Schaels and Hoover (1988), environmental conditions, such as wind and temperature, have great influence on plastic shrinkage cracking of concrete. To reduce plastic shrinkage, the rate of water evaporation should be reduced. Therefore, when there is a high-speed wind, concrete casting should be avoided, or wind breaks and fogging should be used to prevent water loss. Because water evaporation only happens at the surface, plastic shrinkage cracking only occurs at the surface, and it is usually small.

### **2.2.4.2 Autogenous shrinkage**

Autogenous shrinkage happens when the concrete begins to hydrate. It is caused by the self-desiccation of concrete during the hydration process due to lack of water in concrete that has a low water-cement ratio. Autogenous shrinkage is also usually small. But for concrete using high-range-water-reducing admixture (HRWRA) and fine materials, such as silica fume, it may become an important factor leading to shrinkage cracking (Paillere, et al., 1989).

To prevent autogenous shrinkage, low water-cement ratios are not preferred because there is not enough water for the cement to hydrate. When it is necessary to use low water-cement ratio, other methods should be used to compensate for the lack of water due to the low water-cement ratio in the concrete mix design.

#### **2.2.4.3 Drying shrinkage**

Indicated by the pattern of early-age transverse cracking, drying shrinkage cracking is sometime present at bridge decks (Krauss and Rogalla, 1996). It is caused by loss of water in hardened concrete. Drying shrinkage can be explained by three main mechanisms: capillary stress, disjoining pressure and surface tension, each of which plays an important role within a certain range of relative humidity (Mindess, et al., 2003). Normally bridge decks will experience relative humidity from 45% to 90%, when the capillary stress mechanism plays the important role.

Many factors can directly affect the drying shrinkage of concrete, such as paste volume, water-cement ratio, aggregates type, environment conditions and curing methods. Of all these factors, paste volume is the most important one. Drying shrinkage will be greatly reduced if the paste volume is reduced (Xi, et al., 2003; Tritsh, et al., 2005; Darwin, et al., 2007; Delatte, et al., 2007).

#### **2.2.4.4 Test methods of concrete shrinkage**

Many researchers have developed different methods of evaluating the shrinkage cracking tendency of concrete using a wide range of test apparatus. The ring test was most often used one to evaluate the shrinkage cracking tendency and behavior of concrete and cement-based materials under restraint. Tritsch, et al. (2005) divided these restrained shrinkage tests into three categories: plate tests, linear tests, and ring tests.

In the plate tests, flat concrete specimens were tested. Different researchers used different specimen dimensions and different test details. But usually those specimens are thin and the maximum aggregate sizes are small or no coarse aggregates are used. In

some tests the results were inconsistent and conflicted with each other. Free shrinkage tests were also considered as an addition to these restrained tests.

The linear test used specimens of rectangular cross section. Specimens of many different dimensions were used in these tests, such as  $8.5 \times 12 \times 150$  cm ( $3.4 \times 4.7 \times 59$  in.) (Paillère, et al., 1989), and  $40 \times 40 \times 1,000$  cm ( $1.6 \times 1.6 \times 39.4$  in.) (Bloom and Bentur, 1995). In these linear tests, one end of the concrete specimen was fixed, and the other end was connected to an instrument that applies and records the force that is required to keep the specimen in its original length. A companion specimen with the same dimension was also cast, with one end fixed and the other free to shrink, as a control specimen to the restrained one.

Many different concrete rings were tested under a variation of restrained conditions. The dimensions of the concrete ring as well as the test procedure vary greatly from each other. Both the American Association of State Highway and Transportation Officials (AASHTO) and the American Society for Testing and Materials (ASTM) have a developed ring test as one of their standard tests, and they are:

- AASHTO PP34-99. “Practice for Estimating the Crack Tendency of Concrete”.
- ASTM C 1581-04. “Standard Test Method for Determining Age at Cracking and Induced Tensile Stress Characteristics of Mortar and Concrete under Restrained Shrinkage”.

Both the AASHTO Ring Test and the ASTM Ring Test use the same theory and procedures. The main differences between them are the concrete ring dimensions and the maximum size of aggregates allowed. The AASHTO standard concrete ring is 3 in. thick, with inner diameter of 12 in. and outer diameter of 18 in., whereas the ASTM concrete ring is 1.5 in. thick, with inner diameter of 13 in. and outer diameter of 16 in. The ASTM requires that the maximum size of aggregate should be less than 1/2 in., while there is no specific requirement in the AASHTO. Because the concrete ring is thicker in

AASHTO than in ASTM, AASHTO allows greater aggregate size. Also, the duration of the ASTM test is 28 days; while there is no specified duration in AASHTO. Because the AASHTO concrete ring is thicker, it will need more time to crack. Therefore, the AASHTO ring test may typically last for 56 days to 90 days (Delatte, et al., 2007). The curing conditions are also slightly different between the two test methods.

#### **2.2.4.5 Shrinkage test results in the literature**

Limbachiya, et al. (2000) found that the creep and shrinkage strains increase with the RA content in the mix and the creep effect also increases with the reduction in strength. They explained that the increase of creep effect is due to the increased proportion of cement in the RAC. The presence of the attached cementitious paste in RA leads to higher creep and shrinkage in RAC. Hiroshi, et al. (2001) used the decompression and rapid release technique to reduce the creep of RAC so that the creep in RAC was reduced to the same level as NAC. Gomez-Soberon (2002) found that the creep increases with the increasing replacement of NA with RA and presented a formula to describe the relation between the creep and porosity ratio. Ajdukiewicz and Kliszczewicz (2002) conducted the creep and shrinkage tests of RAC over a span of one year, and their results showed that the concrete specimens with 100% of RA have about 35-45% higher of shrinkage, while the creep of RAC is about 20% lower than that of NAC. Katz (2003) performed the drying shrinkage tests of RAC and concluded that the shrinkage could be about 0.55-0.80 mm/m at the age of 90 days, whereas the shrinkage of NAC with the same age is only about 0.30 mm/m. Domingo-Cabo, et al. (2009) studied the influence of replacement ratios of RA on creep and shrinkage, and they found that the evolution of deformation by shrinkage and creep is similar to that of a conventional concrete with NA. When 100% coarse natural aggregate was replaced by RA, the increases in the creep and shrinkage are about 51% and 70%, respectively.

Shrinkage and creep are of considerable importance if RAC is to be used as viable

construction materials. In general, the shrinkage and creep of RAC increase significantly in comparison with NAC, and such increases could be mainly attributed to the old cementitious paste attached to the surface of original NA in RA and the relatively low elastic modulus of RA. When both the fine and coarse RA are used in the RAC mix, the effect of creep and shrinkage will reach the maximum.

### **2.3 Health Monitoring of Concrete Using Piezoelectric Materials**

Although RAC is applicable in civil infrastructure, concrete structures are strong in compression but weak in tension which is likely to cause cracking, aging and deterioration, especially for the structures made of RAC. Consequently, an effective health monitoring technique is needed to assess the condition of RAC structures during their service life so that the economic and human life loss can be avoided. There are many nondestructive methods for inspecting concrete structures, such as radiography, acoustic emission, visual inspection, thermal field, etc. But the limitations of these techniques, including accuracy, cost, maneuverability, in situ capability, etc., make them difficult and/or incapable of being applied to in situ structural health monitoring.

Piezoelectric material, such as Lead zirconate titanate (called PZT), is a kind of smart materials that has been utilized for detecting the defects in concrete structures in recent years. The PZT patches are small, lightweight and inexpensive, and they can be used as both actuators and sensors by considering their piezoelectric effect. In the following, a brief review on damage detection methods of concrete using the elastic wave-based active health monitoring is provided.

Wu and Chang (2006a; b) used the high frequency transient stress waves to detect the debonding damage and its location in a reinforced concrete beam based on a built-in piezoelectric sensors and actuators in a pitch-catch mode. Three types of tests were conducted: debonding tests in reinforced concrete beams, tensile tests on reinforcement

bars, and bending tests of reinforced concrete beams.

Song, et al. (2006; 2008) developed the so-called “smart aggregate” based on piezoceramic patches. The proposed smart aggregate was made by embedding a waterproof piezoelectric patch with lead wires into a small cement block (module). The smart aggregates were then mounted in the desired locations in the concrete molds before the casting of the concrete structures took place. The smart aggregates were used to perform three major tasks: early-age concrete strength monitoring, impact detection, and structural health monitoring. The concrete strength development was monitored by observing the high frequency harmonic wave response of the smart aggregates. The impact on the concrete structure was detected by observing the open-circuit voltage of the piezoceramic patch in the smart aggregates. For the structural health monitoring purposes of concrete, a smart aggregate-based active sensing system was designed, and the wavelet packet analysis was considered as a signal-processing tool to analyze the sensor signal. A damage index based on the wavelet packet analysis was used to determine the structural health status. Their preliminary study demonstrated that the multi-functional smart aggregates have the potential to be applied to comprehensively monitor concrete structures from the earliest age to entire lifetime.

Sun, et al. (2006) used the surface-bonded PZT patches for structural health monitoring of a prism concrete beam. From the velocity of Rayleigh waves and longitudinal waves, the dynamic modulus of elasticity and dynamic Poisson’s ratio of the concrete were obtained. Then, the effect of uniaxial compressive stress and resulting internal cracking of the concrete on the amplitude of the waveforms received by piezoceramic sensors was investigated. The results confirmed that the piezoceramic sensors and corresponding ultrasonic wave methods had the potential to monitor the cracking and long-term deterioration of concrete structures.

Yan, et al. (2009) proposed a smart aggregate-based active sensing approach for

structural health monitoring of a concrete shear wall structure. To evaluate the damage status, the front surface of the shear wall was divided into nine sub-domains. Then, a sweep sinusoidal signal from 100 Hz to 10 kHz was sent by the smart aggregate actuator. A wavelet packet-based damage index matrix was proposed to evaluate the damage status in different sub-domains. The experimental results showed that the proposed smart aggregate-based approach effectively evaluates the damage status in different areas and it is capable of detecting the precautionary point to predict the structural failure.

#### **2.4 Enhanced Performance of RAC with Different Admixtures**

The use of recycled aggregate concrete (RAC) acquires particular interest in transportation infrastructure regarding its sustainable development. Recycled aggregates usually have greater porosity and water absorption, lower density, and lower strength than natural aggregates. Therefore, it is important and beneficial to find potential ways to enhance the RAC performance by seeking different qualified admixtures in casting RAC.

Kou and Poon (2010; 2011) investigated the performance of natural and recycled aggregate concrete with incorporation of different mineral admixtures including silica fumes (SF), meta kaolin (MK), fly ash (FA) and ground granulated blast slag (GGBS). Their test results, in general, showed that the adding of mineral admixtures improved the properties of RAC; the SF and MK contributed to both the short and long-term properties of the concrete. In addition, the results also revealed that the contributions of mineral admixtures to performance improvement of RAC are higher than that to NAC.

On the other hand, the atomic polymer technology (APT) in form of mesoporous inorganic polymer (MIP) can effectively improve material durability and performance of concrete by dramatically increasing inter/intragranular bond strength of concrete at nano-scale. A preliminary study by the PI showed that about 27% in stiffness and 45%

in strength are increased for the concrete with APT.

#### **2.4.1 Atomic polymer technology (APT)**

The strategy of APT is fundamentally different from most additives currently on the market for industrial applications. The atomic polymer changes the nature of the affected chemistry by forming strong chemical and physical bonds to other surfaces within the affected mass. Consequently, there no longer exists any “separate” chemistry, and everything is chemically bonded at the atomic level. When MIP is added to a concrete or masonry mix, this atomic-level bonding means that the strength of the cement or brick mass is defined by the strength of its atomic bonds; these bonds are incredibly strong. Atomic-level bonding also translates the flexibility of the MIP molecule, which is built like a coil, lending strong tensile and flexural strength. Other characteristics of the MIP like fireproofing, self-deicing, antimicrobial features and VOC sequestration are also added.

While MIP itself adds negligible mass into an affected chemistry, it improves and magnifies the beneficial effects on both the basic mix and other additives by creating a ceramic polymer lattice throughout. As a result, it ensures that the physical properties of both the MIP and other additives are translated into the final product with higher efficiency. The following characteristics of the MIP molecule are based on the understanding of the physical chemistry of MIP, as well as a history of materials analysis within a variety of substrates, and observations in the field.

#### **2.4.2 Enhancing mechanism of concrete with APT**

##### ***2.4.2.1 Increased compression and tensile strength***

Changes in the rheology caused by APT allow the concrete form (e.g., portland, pozzolanic, aluminum, or magnesia cements) to act like a liquid and a solid at the same time. This is usually called a “thixotropic” state in which the cement form exhibits a

stable form at rest but becomes fluid when agitated (like custard). The static electrical forces that cause the cement particles and aggregates to be suspended evenly in solution also allow the atomic stacking to take place in their most optimum state. Basically, the static charges hold the atoms in suspended animation, allowing them to find their most optimal atomic binding patterns. While this may slightly delay the cure strength initially, as the atoms take more time to stack properly, the net effect is a much stronger, denser, concrete form. It also makes the cement easier to mold and form.

As stated before, APT uses atomic polymerization to efficiently bind inorganic atoms in the cement to the aggregate. This powerful bonding will increase the compression strength and tensile strength of the concrete. The maximum value of this technology is gained when pretreating the aggregate for about 10 minutes to allow the absorption and full adherence of MIP into the pores of the aggregate.

#### **2.4.2.2 Increased durability**

The MIP's patented Active Cure Technology (dewatering function) also affects the ability of ice crystals to form as it is basically always pulling water molecules apart. In order to form ice crystals, water molecules have to be still and lose sufficient heat energy to transition to their solid phase, ice. This disturbance of the water's molecular bonds has the effect of interfering with ice-crystal formation, thereby stopping ice formation on the surface of the cement. This phenomenon will occur even when MIP is bound in the concrete mass, as not all the quadpore locations will be bound by the concrete matrix. This effect is regulated by the amount of MIP added to the matrix and the amount of surface area interacting with MIP in the concrete matrix (certain additives like silica fume dust are likely to adhere more of MIP and may lessen the effect at the surface).

On the other hand, MIP is exceptionally statically charged and will act as a strong ionic emulsifier within the concrete matrix. The aggregate, especially the fines (including fume dust and other densifiers) will be evenly suspended in solution. This

effect will increase the workability of the concrete, while also adding to the efficiency of the aggregate space filling process, leading to stronger overall concrete.

The effects of MIP on the above two mentioned physical properties will increase the durability of the concrete as there are decreased freeze-thaw damage and decreased damage from expansion-contraction episodes due to cold and heat extremes. It is thus anticipated that the inclusion of MIP in recycle aggregate concrete (RAC) can effectively improve its performance and long term durability.

## **Chapter 3 Test Programs for Recycled Aggregate Concrete**

This chapter describes the test methods considered in this study for the shrinkage and smart health monitoring of the RAC.

### **3.1 Free Shrinkage Test**

The free shrinkage test was performed according to AASHTO T 160 (ASTM C 157) “Length Change of Hardened Hydraulic Cement Mortar and Concrete”. The dimension of the test samples are  $4 \times 4 \times 11.25$  in. ( $101.6 \times 101.6 \times 285.75$  mm). All the prisms were demolded at 24 hours after casting and moved to the condition room for testing. The condition room was maintained at a temperature of  $76 \pm 3^{\circ}\text{F}$  and a relative humidity of  $50 \pm 4\%$ . Each prism specimen was supported by two steel roller bar in order that it is able to shrink free of abrasion. In addition, the frame was installed in an inclined slope with a small angle by supporting one side of the frame with a wood stack. With this setup, one end of the tested specimen always keeps in touch with the frame while the other end deforms freely such that the free shrinkage could be measured as accurate as possible.

### **3.2 Restrained Free Shrinkage Test**

As aforementioned, the ring test method was used to evaluate the relative drying shrinkage cracking tendency of different concrete mixes under different conditions. The ring test restrains the concrete using a steel ring, thus inducing a stress on the surrounding concrete ring. When this stress becomes larger than the tensile strength of the concrete, the concrete ring will crack. The time that it takes for rings with different amounts of APT to crack are recorded and then compared with each other. The longer it takes a concrete ring specimen to crack, the lower tendency of drying shrinkage cracking it has.

The ring test is simple and easy to conduct. Also, it evaluates most of the important factors that affect the drying shrinkage cracking tendency at one time. Furthermore, the cracking in the concrete ring can be easily recognized and recorded. Therefore, the ring test method has become the most popular method for evaluating the restrained drying shrinkage of concrete.

Considering that the maximum size of RA used in this study is around 1.25 in., the AASHTO PP34-99 “Estimating the Cracking Tendency of Concrete” was adopted in this study. Structural steel pipe conforming to ASTM A 501 or A 53M/A 53 12-in. extra-strong pipe with an outside diameter of 324 mm (12 ¾ in.) and wall thickness 13 mm ( 1/2 in.) was used for fabricating the inner steel ring (**Figure 3.1**). The outer ring was made of polyethylene board with an inside diameter of 457 mm (18 in.). Four strain gages were mounted on the inner surface of the steel ring at equidistant points at midheight (see **Figure 3.1**).

The outer forms of the ring molds were removed at an age of 8 hour, and then all specimens will be moved to the conditional room with a constant air temperature of  $76 \pm 3^{\circ}\text{F}$  and a relative humidity of  $50 \pm 4\%$ . Data acquisition equipment from Vishay Company was used for the strain instrumentation, and it automatically records each strain gage every second independently. The data from the strain gages was recorded every half an hour, and review of the strain and visual inspection of cracking was conducted every 2 or 3 days.

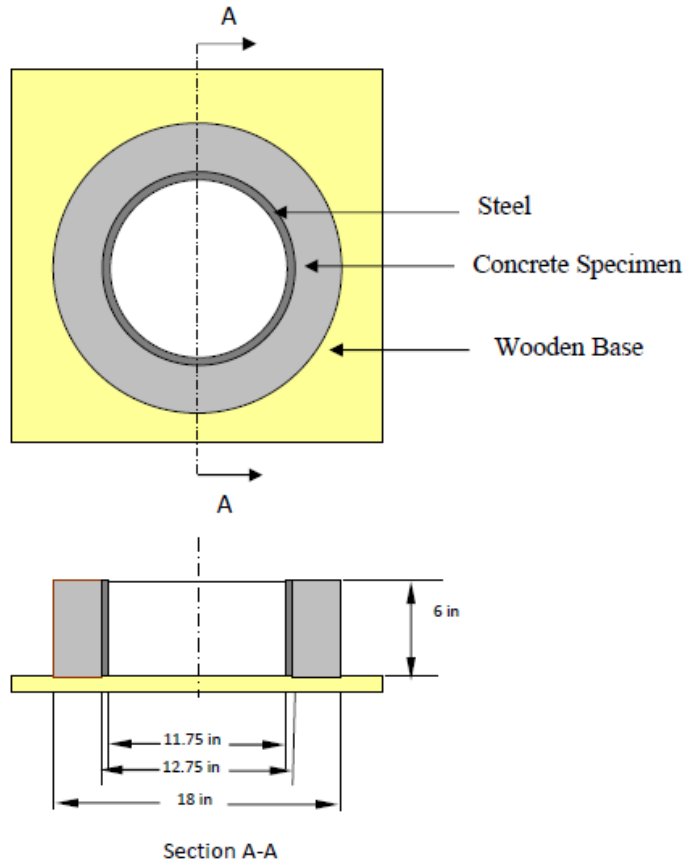


**Figure 3.1 Diagrams of Ring Specimen Used (Reprinted from AASHTO PP34-99).**

### 3.3 Dynamic Modulus Test

Modal testing is a nondestructive method for assessing the dynamic response of structures. This method uses sinusoidal excitation for the input signal and forces the specimen to vibrate at a frequency while the response of the specimen is monitored with an accelerometer. In this study, the dynamic modulus test was adopted to measure the stiffness gaining process of RAC during its curing period.

ASTM C215 uses modal testing to assess degradation to beams/prisms undergoing freezing-thawing (F/T) conditioning. A natural frequency of vibration is a characteristic (dynamic property) of the tested elastic system. Assuming that the concrete samples are homogeneous, isotropic, elastic material, the dynamic modulus of concrete is thus related to the resonant frequency and density. According to ASTM C215, two methods for

measuring resonant frequency are sinusoidal excitation (forced oscillation) and impact excitation. The classic forced resonance setup uses either transverse or longitudinal resonance. In the longitudinal mode, the oscillator is at one end and the pickup is at the other. In the transverse mode, the oscillator is in the middle of the top surface, and the pickup is at one end of the top surface. The ASTM C215 impact method uses a modally-tuned impact hammer to excite vibrations in the tested beam and an accelerometer attached to the beam to record the response. Modal tuning enables the isolation of the hammer's response from the structural response, thus providing an accurate measurement of the specimen response, rather than the combined system (impact hammer and structure) response.

In this study, the dynamic modulus test was conducted following ASTM C215. The fundamental transverse frequency was tested to calculate the dynamic modulus of elasticity of the samples under certain F/T cycles. The impact test method was used to measure the transverse frequency, where an accelerometer (output signal) was attached to one end of the beam using vacuum grease. The test sample was slightly knocked by the impact hammer at the approximate middle of the sample. The time domain response data (impulse versus time and response versus time) were recorded automatically by the commercial software "Control Desk". Typical time domain impulse and response data are shown in **Figure 3.2** and **Figure 3.3**, respectively. The frequency domain response data are shown in **Figure 3.4**.

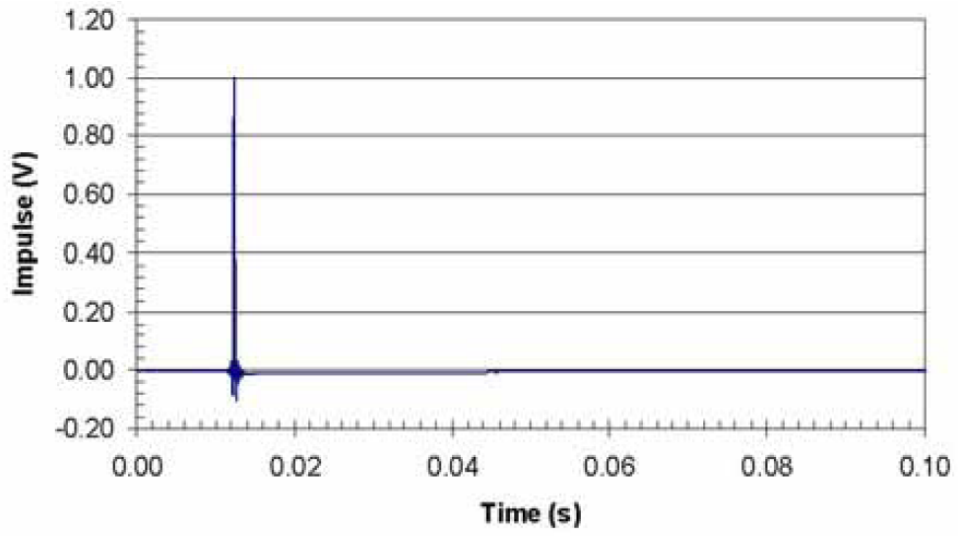


**Figure 3.2 Time Domain Impulse Signal.**

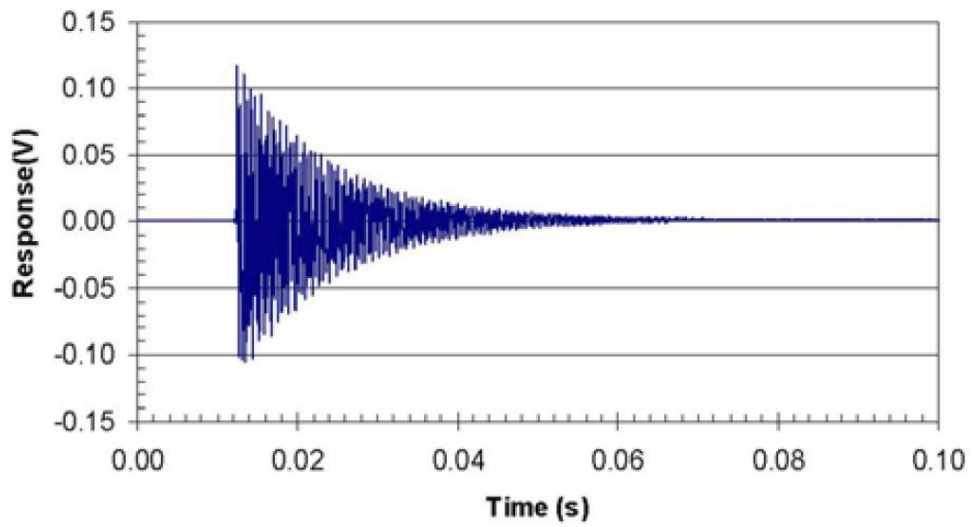


**Figure 3.3 Time Domain Response Data.**

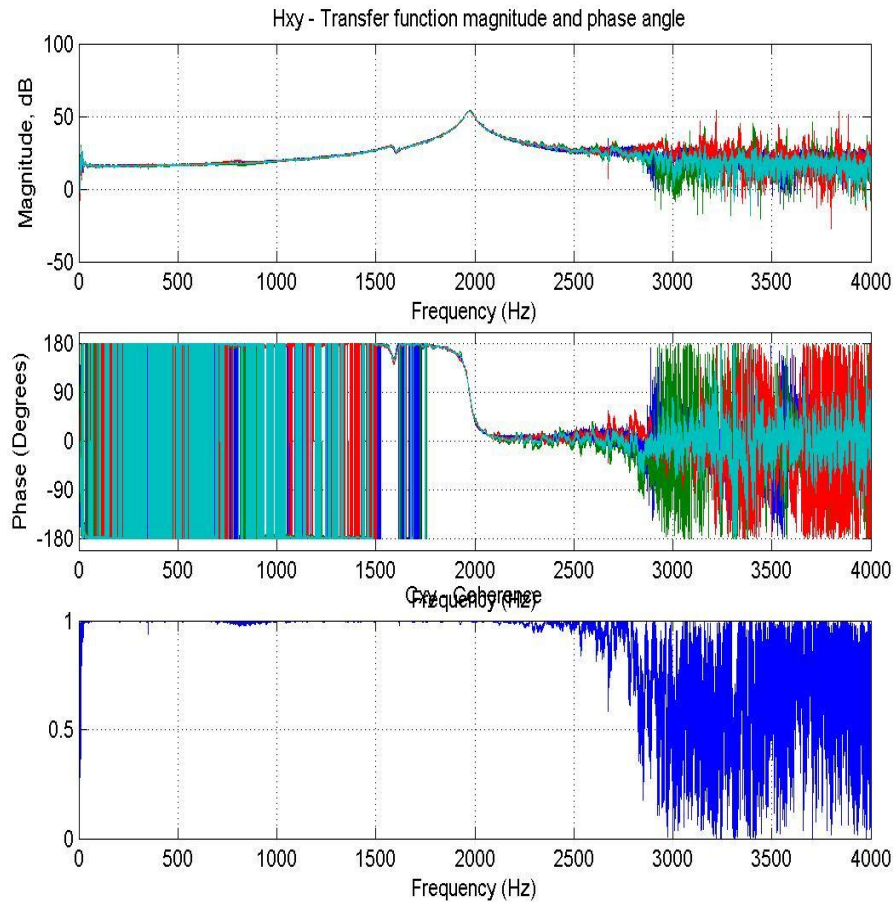
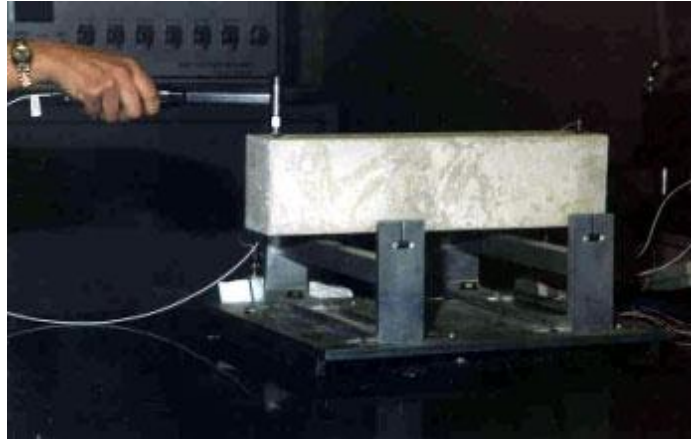
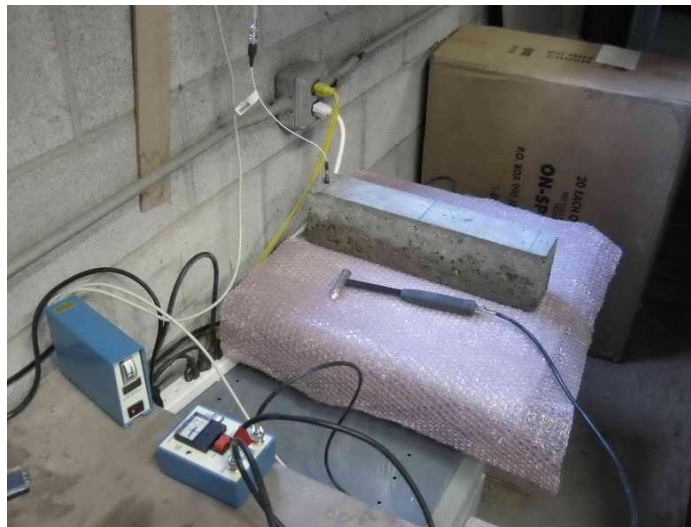


**Figure 3.4 Frequency Domain Response Data.**

According to ASTM C215, the test samples should be supported at locations with distance of about 0.224 of the length of the sample from each end so that it is able to vibrate freely in the transverse mode as shown in **Figure 3.5a**. However, based on the test data from an alternative support approach where the sample was placed on a thick pad of soft sponge (as shown in **Figure 3.5(b)**), the results of these two different supporting methods were compared and it was found that the difference of these two approaches is about 0.02-0.05%. Considering the simplicity of the second support method, the thick pad support approach was used in this study for the transverse frequency test.



(a) Test support suggest by ASTM C215



(b) Thick pad support approach used in this study

**Figure 3.5 Setup for Dynamic Modulus Test.**

The dynamic Young's modulus of elasticity,  $E_d$ , in Pascal, can be determined from the fundamental transverse frequency, mass, and dimensions of the test sample, and the definition equation is as follows:

$$E_d = CMn^2 \quad (3.1)$$

where  $M$  is the mass of the sample;  $n$  the fundamental transverse frequency;  $C = 0.9464T \frac{L^3}{bt^3}$  for a prism;  $L$  length of the sample;  $t$  and  $b$  thickness and width of the

sample;  $T$  correction factor that depends on the ratio of the radius of gyration to the length of the specimen and the Poisson's ratio, according to the ASTM C215 standard, and considering the samples used in this study, the value of  $T$  is chosen as  $T = 1.41$ .

### 3.4 Elastic wave-based method

In this study, the elastic wave propagation-based technique was also adopted to develop health monitoring techniques for concrete embedded with smart aggregates. It is expected that with the increase of the curing time of RAC, the earlier stiffness of the RAC will keep increasing. Therefore, the stiffness gaining process of the RAC in term of the modulus of elasticity (MOE) could be monitored by evaluating the change of the modulus of elasticity (MOE) of concrete over time.

The wave propagation tests were conducted using the smart aggregates embedded at the locations near the two ends (one serving as actuator, and the other as sensor) for health monitoring. The smart aggregate was located at about 1 in. (25.4 mm) from the end of the beam. An Agilent 33120A function generator was used to generate the tone burst excitation signal (see **Figure 3.6**). The excitation signal was a 3.5 cycles 100 kHz sine wave windowed by a Hanning window, as shown in **Figure 3.7**. The stress wave package was generated by the embedded smart aggregate at one end, and the response signal was captured by the smart aggregate at the other end. Since the in-plane dimension of the thin square PZT plate actuator in its plane is much larger than its thickness, the major effect of PZT actuation is perpendicular to the beam length direction.

As an attempt to quantitatively investigate the extent of damage or degradation induced by the F/T conditioning, the first stress wave package was investigated. This wave package obviously travels from one actuator at one beam end to a sensor at the other beam end in a straight line. The time of flight (*TOF*) of the wave package can be easily identified by the time interval between the peaks of the excitation signal energy

and response signal energy.

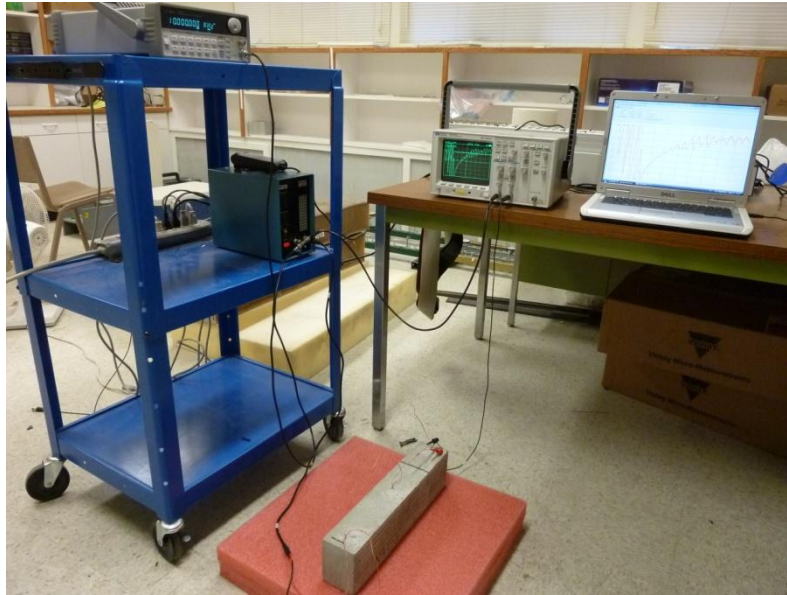


**Figure 3.6 Experimental Setup for Health Monitoring of RAC Prism in Smart Structures Lab at WSU.**

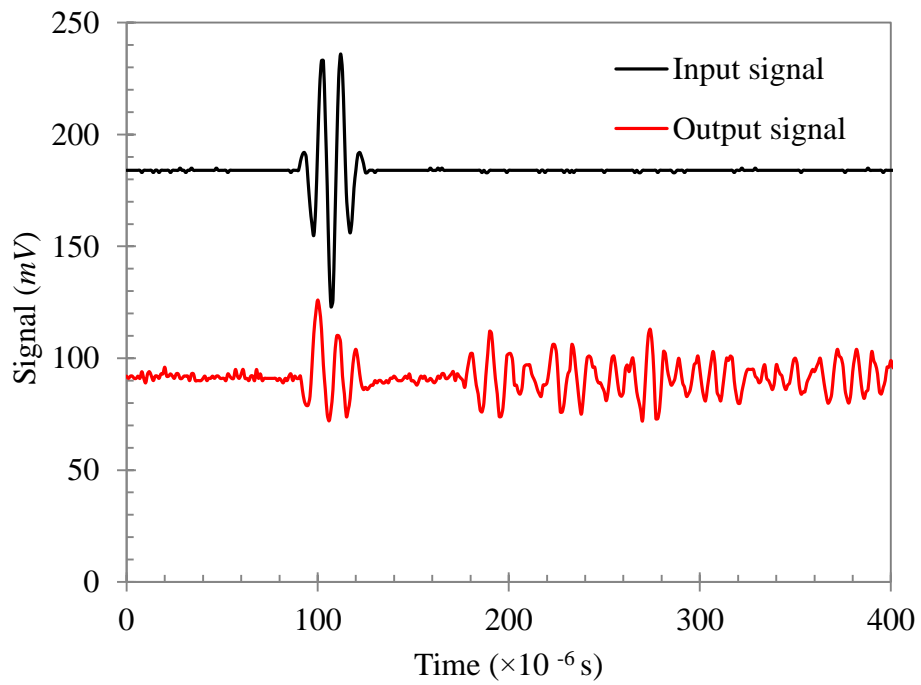


**Figure 3.7 Input and Output Signals Captured by Smart Aggregate.**

The speed of shear wave ( $C_s$ ) inside the concrete can be predicted by

$$C_s = \sqrt{\frac{E_w}{2(1+\nu)\rho}} \quad (3.2)$$

where  $E_w$  represents the modulus of elasticity (MOE) of concrete based on the wave test ;  $\rho$  is the density of concrete;  $\nu$  is the Poisson's ratio of concrete.

From the speed of shear wave, the time of flight ( $TOF$ ) of the first shear wave package can be predicted by

$$TOF = l / C_s \quad (3.3)$$

where  $l$  is the given distance between the actuator and sensor.

Based on Eqs. (3.2) and (3.3) and assuming that the Poisson's ratio and density of the concrete keep unchanged during curing time, the following relationship can be established between the  $TOF$  and  $E_w$  of the concrete samples:

$$TOF \propto \frac{1}{C_s} \propto \frac{1}{\sqrt{E_w}} \quad (3.4)$$

Thus, based on the change of the measured  $TOF$ , the variance of  $E_w$  can be obtained at different time, from which the strength/stiffness gaining of RAC during its curing period can be monitored and assessed.

## Chapter 4 Materials and Sample Fabrication

### 4.1 Materials and Mix Design

#### 4.1.1 Aggregates

Recycled coarse aggregates were provided by Central Pre-Mix Concrete Company in Spokane, WA, and they contain 30% of virgin (normal) aggregates. The gradations of the recycled coarse aggregates are presented in **Table 4.1**. The specific gravities and water absorption of both the recycled aggregate (RA) alone (100% of RA) and virgin aggregate are listed in **Table 4.2**. The maximum normal size of RA is about 1-1/4 in. (31.75 mm).



**Figure 4.1 Recycled Aggregates.**

Natural fine aggregates were also provided by Central Pre-Mix Concrete Company in Spokane, WA. The fine aggregates meet Class 1 WSDOT Sand requirements. The specific gravity of fine aggregates is also listed in **Table 4.2**, and the detailed gradation is given in **Table 4.3**.

**Table 4.1 Coarse Recycled Aggregate Gradations (Sieve Analysis)**

	Recycled Aggregate 1-1/4"
Sieves	Cumulative % Passing
1-1/4"	99.1
1"	87.8
3/4"	70.3
5/8"	56.5
1/2"	39.2
3/8"	25.2
1/4"	5.9

**Table 4.2 Specific Gravity and Water Absorption of the 1-1/4" Recycled Aggregates**

Aggregates	Recycled Aggregate	Virgin Aggregate	Sand
Specific Gravity	2.32	2.68	2.65
Absorption	7.4%	1.2%	-

**Table 4.3 Fine Aggregate Gradation (Sieve Analysis)**

Sieves	Fine Aggregate	
	Individual % Retained	Cumulative % Passing
3/8"	0	100
1/4"	0.5	99.5
#4	1.8	97.7
#8	13.4	84.3
#16	23.3	61
#30	18.8	42.2
#50	24.5	17.7
#100	13.6	4.1
#200	1.9	2.2

#### **4.1.2 Chemical admixtures**

Three types of chemical admixtures, air entraining admixture (AEA), high range water reducing admixture (HRWRA), and super-plasticizers, were used in this study to obtain the desired workability.

DARAVAIR 1000 air-entraining admixture from Grace Construction Products was used to ensure proper air content in all the concrete mixes. According to the information from the product instructions, it is based on a high-grade saponified rosin formulation and chemically similar to vinsol-based products. The rational admixture range of the chemical admixtures is shown in **Table 4.4**. The actual adding amount was determined by the recommended addition rate from the product instructions and adjusted during concrete casting.

ADVA 64 and Super plasticizer ADVA 100, high-range water-reducing admixtures from Grace Construction Products, were adopted to achieve the desired slump value as well as reducing the water content in all concrete mixes. They are polycarboxylate-based admixture specifically designed for concrete industry and conform to the requirements of ASTM C 494 as a Type F admixture. Their adding rate were also determined according to the product instructions and adjusted by practice.

**Table 4.4 Rational Chemical Admixture Range**

	Air entraining	Atomic polymer	Super plasticizer ADVA 100	ADVA 64
Range	0-24 ml	192,320,448 ml (3,5,7 oz/ gallon water)	10-70 ml	23-91 ml

#### 4.1.3 Mix designs

A standard WSDOT mix design was applied in this study. The mix designs for RAC considered in this study are summarized in **Table 4.5**, and the actual amount of chemical admixtures added in different mixture batches are shown in **Table 4.6**. Three mix designs were designed to evaluate the effect of inclusion of APT on the performance of RAC: (1) Batch#1: Standard WSDOT mix without inclusion of APT, (2) Batch#2: Standard WSDOT mix with inclusion of 3 oz. APT per gallon of water, and (3) Batch#3: Standard WSDOT mix with inclusion of 5 oz. APT per gallon of water. During the concrete mixing, half of APT was first mixed with water and then poured into the mixer to wet the coarse aggregates, and the rest half of APT was added into the mixer after three minutes mixing.

**Table 4.5 WSDOT Mix #0948 with and without APT**

Cement (lb/yd <sup>3</sup> )	Fly Ash (lb/yd <sup>3</sup> )	1-1/4" Recycled Aggregate (lb/yd <sup>3</sup> )	Sand (lb/yd <sup>3</sup> )	w/cm	Air Content (%)	Water (lb)
660	75	1730	1250	0.34	6.5	250

**Table 4.6 Chemical Admixtures in Different Batches**

Batch	Air entraining	Atomic polymer	Super-plasticizer ADVA 100	ADVA 64
Batch #1 WSDOT	25 ml	0 ml	65 ml	0 ml
Batch #2 3oz/gallon	25 ml	192 ml	65 ml	100 ml
Batch #3 5oz/gallon	25 ml	320 ml	95 ml	100 ml

#### 4.2 Smart Aggregates Fabrication

The smart aggregates are small cement module (cylinder) (about 3/4" (19.05 mm) in diameter and 3/4" (19.05 mm) in thickness) with embedded thin rectangular PZT patches (plates). The size of the PZT patch used in this study is 0.5" × 0.5". (12.7 × 12.7 mm). The PZT patch was first soldered with two wires as conductors, and then coated with a thin layer of insulating/waterproofing coating from GC Electronics as shown in **Figure 4.2**. The coated PZT patches were then embedded in cement modules to form the so-called "smart aggregates" (see **Figure 4.3**). These modules were made from a mixture of cement, sand and water (cement: sand: water = 1: 1.5: 0.48 in weight), and they were cast using a plastic mold (see **Figure 4.4**). To minimize the noise effect from the electromagnetic interference (EMI) caused by the high voltage excitation signal on the response signal, the smart aggregates were further insulated by bonding the isolant electric tape in a crossing way as shown in **Figure 4.5**. Eventually, the isolated smart aggregates were embedded into concrete beams to serve as both actuators and sensors for

active health monitoring.

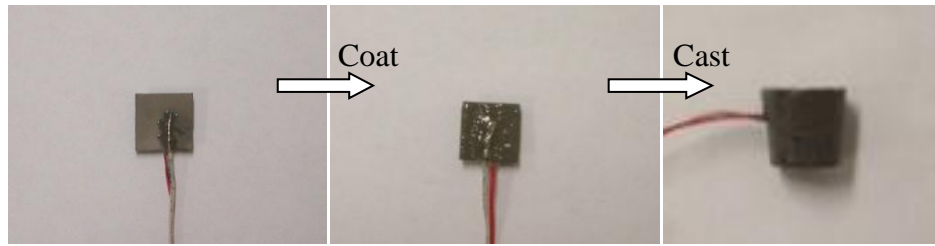


**Figure 4.2 Fabrication Process of Smart Aggregate.**

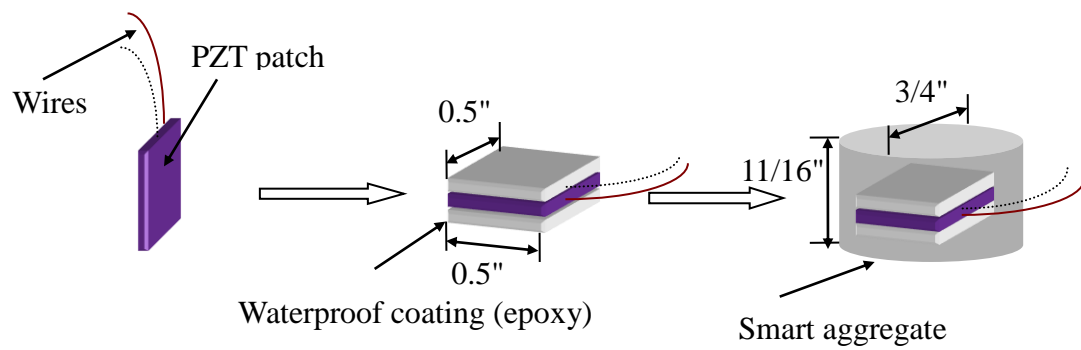


**Figure 4.3 Schematic of Fabrication Process of Smart Aggregate.**

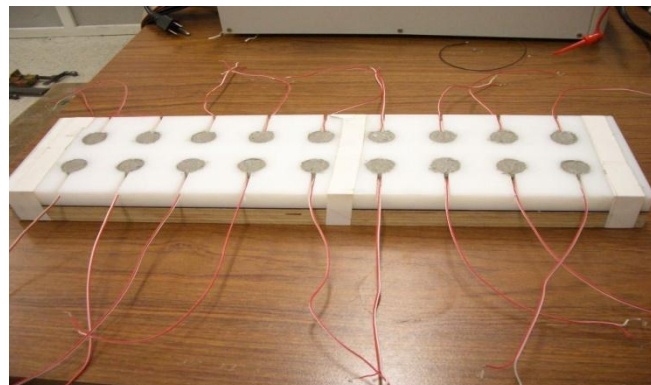
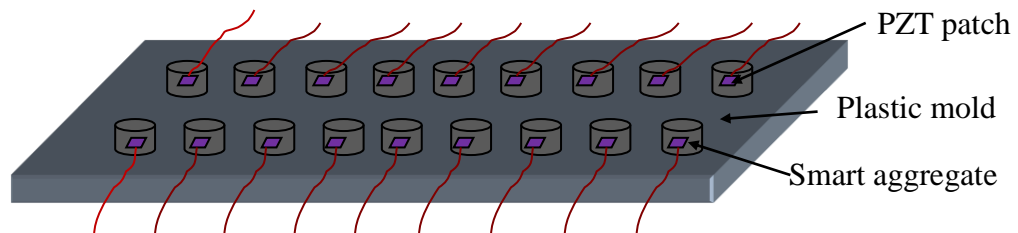


**Figure 4.4 Plastic Mold for Fabrication of Smart Aggregate Concrete Mixing and Sample Preparations.**

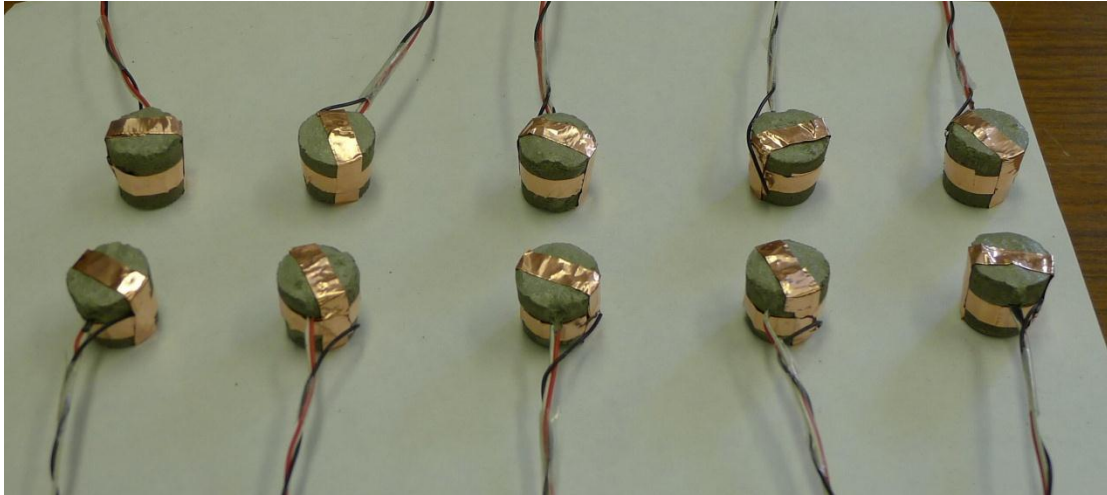


**Figure 4.5 Isolation of Smart Aggregates with Electric Tapes.**

### **4.3 Concrete Mixing and Sample Preparation**

All concrete mixing and sampling were conducted in the concrete laboratory of the department of Civil and Environmental Engineering, Washington State University. Concrete mixing and sample casting strictly followed the ASTM standard: C31/C31M-10 Standard Practice for Making and Curing Concrete Test Specimens in the Field.

#### **4.3.1 Concrete beam samples with embedded smart aggregates**

Three groups (with 0 oz, 3 oz and 5 oz APT) and a total of nine concrete beam samples with dimensions of  $3 \times 4 \times 16$  in. ( $76.2 \times 101.6 \times 406.4$  mm) were cast for monitoring stiffness gaining process during its curing stage. Two “smart aggregates” were mounted in the mold before casting, and a concrete beam sample with the embedded smart aggregates are shown in **Figure 4.6**. The smart aggregate was located at about 1 in. (25.4 mm) from the end of the beam. After all beam samples were demolded, the stiffness gaining of the concrete samples during its curing process was monitored immediately through the wave test at an interval of 24 hours. At the meantime, the dynamic modulus test was also conducted to measure the modulus variance at every 24 hours. After each test, all samples were cured in saturated lime water at room temperature. The monitoring

of the stiffness gaining process of the concrete beam samples with different amount of APT was conducted till 28 days for both the elastic wave-based test and dynamic modulus test.

### 4.3.2 Concrete ring samples

To fabricate the concrete ring models, wooden forms were made of  $24 \times 24 \times 5/8$  in. ( $0.6 \times 0.6 \times 0.016$  m) plywood sheet, and the top surface was coated with epoxy such that the concrete rings are able to shrinkage freely. The preparation of strain gages on the steel rings consists of three steps and strictly follows the recommendation of Vishay Micro-Measurements group: (1) the surface preparation, (2) the strain gage installation, and (3) the wire attachment. The prepared rings are shown in **Figure 4.7**.

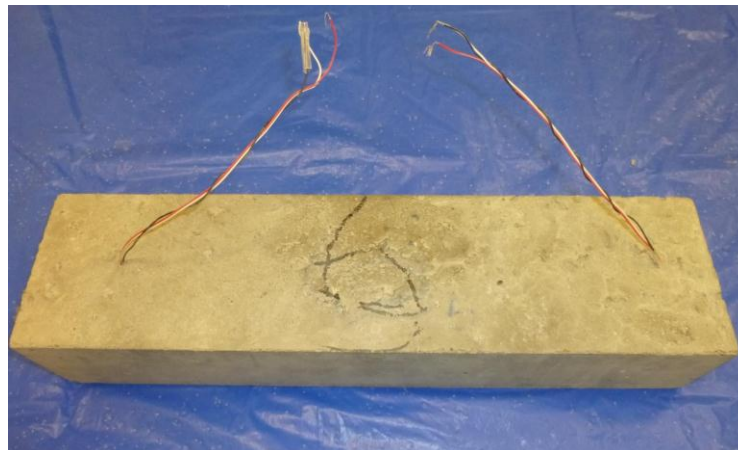
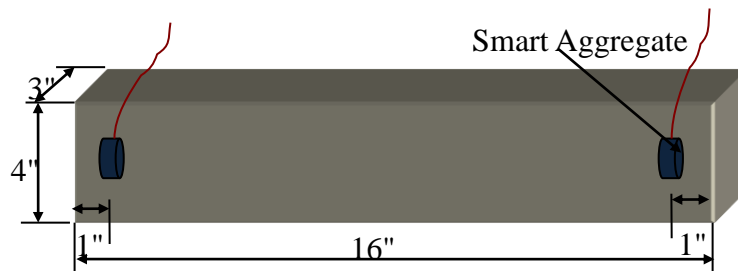


**Figure 4.6 Concrete Beam Specimen and Placement of Embedded Smart Aggregates.**



**Figure 4.7 Restrained Shrinkage Ring Apparatus.**

A total of six ring specimens were cast (with two samples at each group). The concrete specimens were placed in the molds in three equal lifts and consolidated by using a vibrating table. All samples were sealed with plastic at the top surfaces to prevent loss of moisture (see Figure 4.8), and the outer forms were removed at an age of 8 hours. Then, all the specimens were moved to the conditional room (see **Figure 4.9**) with a constant air temperature of  $75 \pm 3.5$  and  $50 \pm 4$  % relative humidity. The data from the strain gages were recorded every half an hour and review of the strain and visual inspection of cracking were conducted every day.



**Figure 4.8. Top Surface Sealing of the Ring Samples.**



**Figure 4.9 Ring Test Setup in the Condition Room.**

## Chapter 5 Test Results and Analysis

To characterize the material behavior and quality of the concrete, basic material property tests for both fresh and hardened concrete were conducted, and their procedures are briefly explained in the following sections.

### 5.1 Test Results for Fresh Concrete

Slump and air content tests were performed on fresh concrete to evaluate the workability and durability properties. The slump test was conducted following the procedures of ASTM C 143/AASHTO T 119 “Slump of Hydraulic Cement Concrete”, and the air content test was conducted following the procedures of AASHTO T 152/ASTM C 231 “Air Content of Freshly-mixed Concrete by the Pressure Method” (see **Figure 5.1**).



**Figure 5.1 Slump Test of Fresh RAC.**



**Figure 5.2 Air Content Test.**

The slump and air content for the concrete with different amounts of APT (i.e., 0, 3 oz., and 5 oz. per gallon of water) are listed in **Table 5.1**. The slump values are in the range of 4.5 to 6.5 in., which indicates good workability of all the samples with different amounts of APT. The air contents are also within the desired range for most of the concrete mixes.

**Table 5.1 Material Properties of Fresh Concrete**

Mixtures	Slump (in.)	Air Content (%)
WSDOT (0 oz APT)	5.6	6.5
3 oz APT	4.8	5.4
5 oz APT	6.3	4.6

## 5.2 Test Results for Hardened Concrete

Three basic mechanical properties were evaluated for the hardened concrete:

compressive strength, modulus of elasticity, and flexural strength. The compressive strength test (**Figure 5.3**) was conducted following the procedures of ASTM C 39/AASHTO T 22 “Compressive Strength of Cylindrical Concrete Specimens”; the modulus of elasticity test (**Figure 5.3**) was conducted following the procedures of ASTM C469 “Standard Test Method for Static Modulus of Elasticity and Poisson's Ratio of Concrete in Compression”; while the flexural strength test (Figure 5.4) was performed following AASHTO T 97/ASTM C 78 “Standard Method of Test for Flexural Strength of Concrete (Using Simple Beam with Third-Point Loading)”.



**Figure 5.3 Compressive and Modulus of Elasticity Test.**



### Figure 5.4 Flexural Strength Test.

The Young's modulus, compressive strength and flexural strength of concrete samples with three different amounts of APT (i.e., 0, 3 oz., and 5 oz. per gallon of water) are shown in **Table 5.2**. It can be seen from **Table 5.2** that both the Young's modulus and strength of the RAC increase as the increase of the added APT, among which the compressive strength at 7 days increased as much as 42% by adding 5 oz APT/gallon into the RAC. This indicates that the APT is a qualified and promising admixture to effectively improve material properties in terms of Young's modulus and strength of RAC. The dramatically-increased compressive strength as shown in **Table 5.2** on the other hand demonstrates that the strengthened atomic-level bonding due to the added APT governs the macro-level compressive strength.

**Table 5.2 Material Properties of Hardened Concrete**

		0 oz APT	3 oz APT	% increase	5oz APT	% increase
Young's modulus ( $\times 10^6$ psi)	7 days	2.92	3.29	12.7	3.76	28.8
	28 days	3.25	3.84	18.2	3.98	22.5
Compressive strength (psi)	7 days	4028.0	4692.8	16.5	5717.8	42.0
	28 days	4958.7	5859.4	18.2	6649.1	34.1
Flexural Strength (psi)	7 days	562.1	592.2	5.4	644.5	14.7
	28 days	664.4	675.0	1.6	812.6	22.3

### 5.3 Dynamic Modulus Test Results

The fundamental transverse frequency was tested to calculate the dynamic modulus of elasticity ( $E_d$ ) of the RAC samples during the curing period and to examine the developing stiffness/strength. During the curing stage, the dynamic MOE tests were conducted in an interval of 24 hours until 7 days and then in an interval of 3 days till 27

days. The variances of frequency and  $E_d$  with respect to the curing time are compared in **Figure 5.5** and **Figure 5.6**, respectively. It can be seen from **Figure 5.5** and **Figure 5.6** that the frequency and dynamic MOE gradually increase for all RAC samples with the increase of the curing time, indicating that the samples are gaining stiffness and strength, and the increased frequency and dynamic modulus during the first half curing time (i.e., the first 15 days) is much larger than those in the rest of the curing time. However, as shown in **Figure 5.5** and **Figure 5.6**, the frequency and dynamic modulus of the RAC does not increased considerably with the increase of the added APT, indicating that the effect of APT on the global dynamic modulus of the RAC is not as obvious as that on the Young's modulus based on the compressive test.

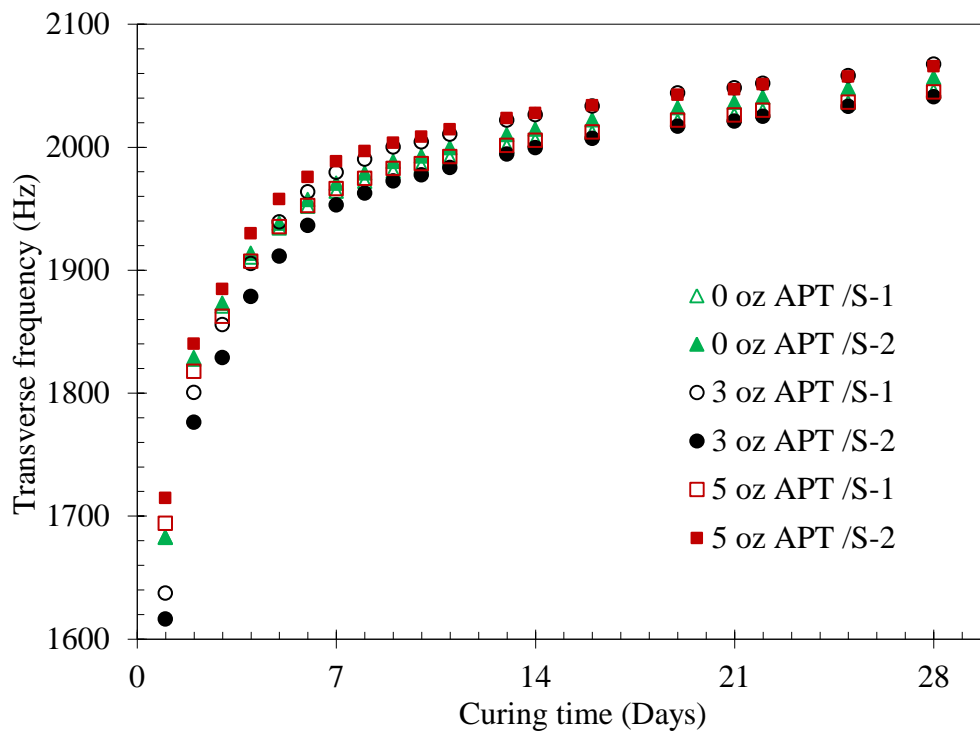


**Figure 5.5 Variance of Frequency with Respect to Curing Time.**

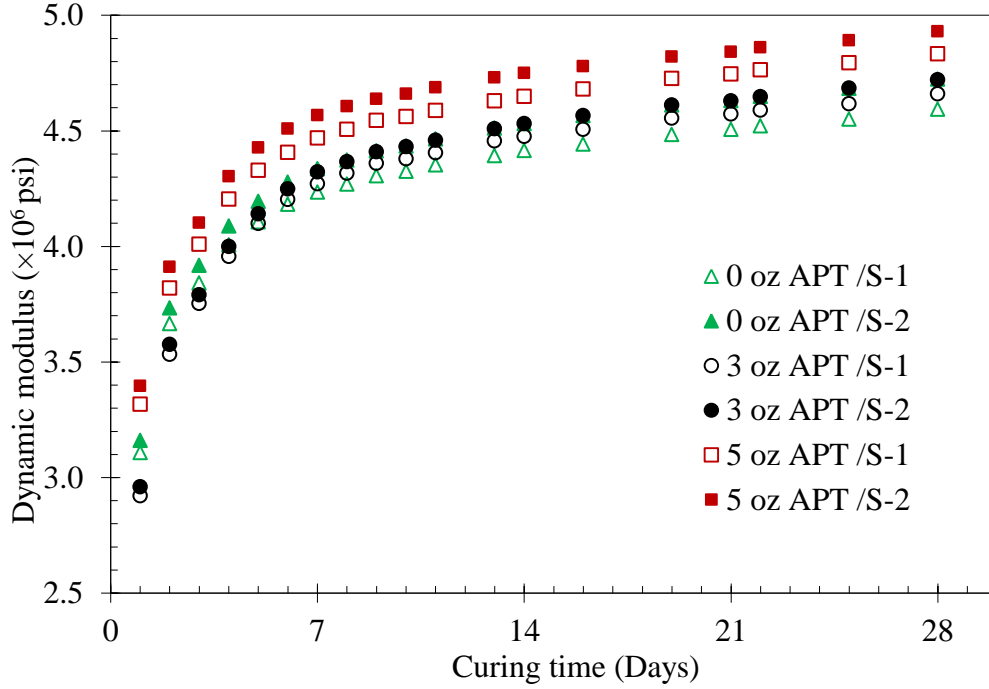


**Figure 5.6 Variance of Dynamic MOE with Respect to Curing Time.**

#### 5.4 Modulus of Elasticity Based on Wave Test Results

In this section, the RAC beam samples with the embedded smart aggregates and their health condition in term of the modulus of elasticity (MOE) was monitored with the embedded smart aggregates by the time of flight (*TOF*). The *TOF* of the 1<sup>st</sup> shear wave package was measured to calculate the variance of  $E_w$ . Assuming that the Poisson's ratio and density of the RAC beams keep unchanged during the curing time, the relationship between the *TOF* and MOE of the RAC samples was used to monitor (or measure) the change of MOE over the time.

First, the original signal from the actuator was collected. The *TOF* of the 1<sup>st</sup> shear wave package in the healthy state was then identified. The absolute value of the MOE based on wave test ( $E_w$ ) and shear modulus ( $G_w$ ) can be obtained using Eqs (5.1) and (5.2), assuming the Poisson's ratio to be constant at 0.15.

$$E_w = 2(1+\nu)\rho C_s^2 \quad (5.1)$$

$$G_w = \rho C_s^2 \quad (5.2)$$

The variances of  $E_w$  and  $G_w$  with respect to the curing time are shown in **Figure 5.7** and **Figure 5.6**, respectively. Similar to the dynamic modulus, the modulus of elasticity (MOE) based on the elastic wave test also gradually increase for all RAC samples during the curing period. It should be mentioned that, due to the electromagnetic interference (EMI) caused by the high voltage excitation signal, the variance trends of the reduced modulus over the curing time based on the wave test data were not as smooth as those of the dynamic modulus based on the dynamic modulus test. However, the effect of the inclusion of APT on the RAC stiffness can be obviously observed based on this elastic wave test, as noticed by the significant increase of both the extension and shear modulus (as shown in **Figure 5.7** and **Figure 5.6**) with respect to the increase of APT.

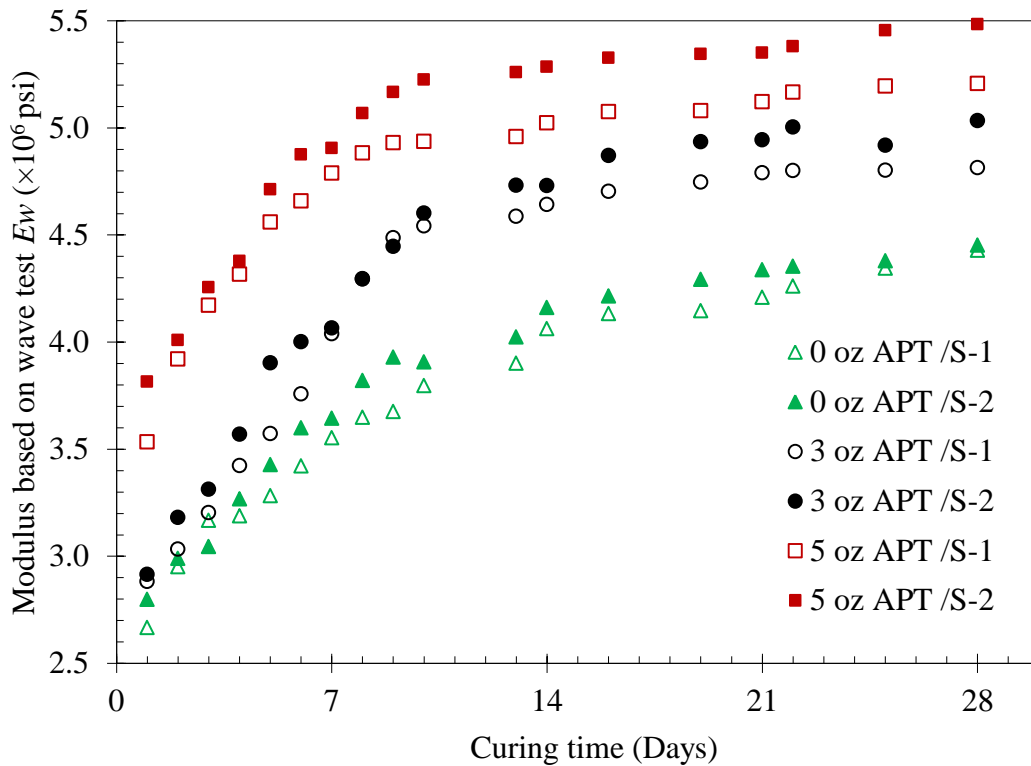


**Figure 5.7 Variance of  $E_w$  with Respect to Curing Time.**

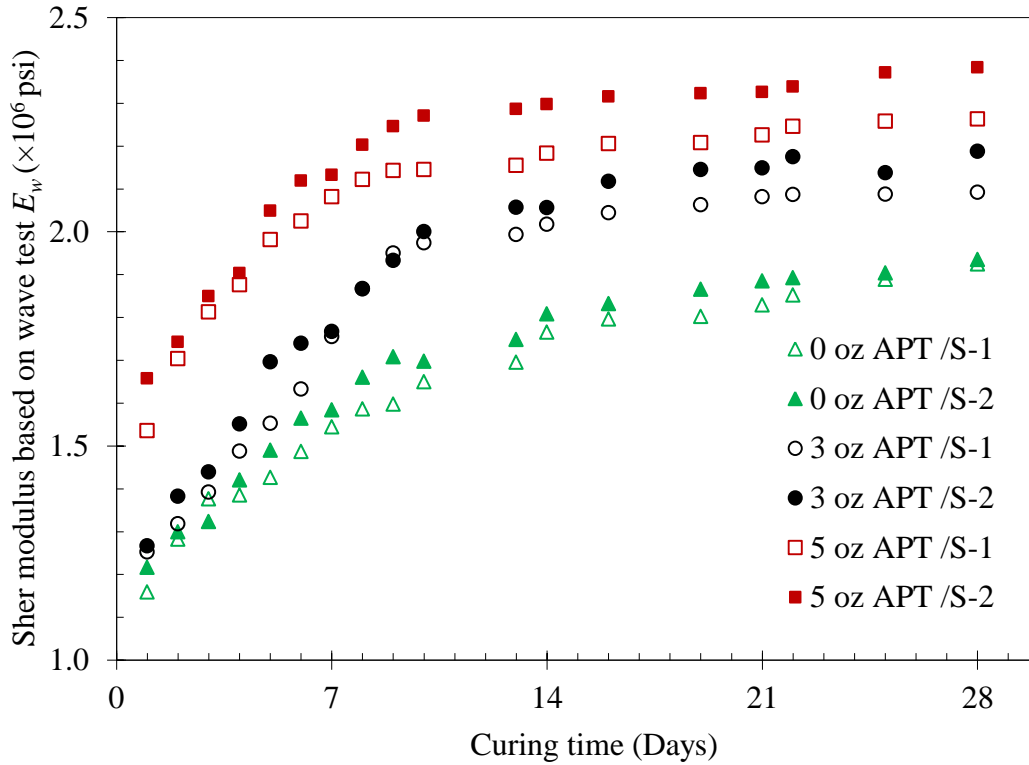


Figure 5.8 Variance of  $G_w$  with Respect to Curing Time.

### 5.5 Comparisons of modulus of elasticity among different test methods

The elastic modulus of the studied RAC samples added with different amounts of APT and determined by different test methods (i.e., static compressive test, dynamic modulus test, and elastic wave-based test) are compared in **Table 5.3**. As shown in **Table 5.3**, the elastic modulus measured by the elastic wave test generally produced the highest value, followed by the dynamic modulus test and then the compression test.

**Table 5.3 Modulus of Elasticity by Different Methods at 7 and 28 days**

Curing Times (Days)	Mixtures		Compr. test	Average ( $\times 10^6$ psi)	Dynamic modulus test	Average ( $\times 10^6$ psi)	Elastic wave test	Average ( $\times 10^6$ psi)
7 day	0 oz	S-1	2.956	2.916	4.235	4.286	3.553	3.599
		APT	S-2		2.751		4.337	
	3 oz	S-1	3.163	3.297	4.271	4.297	4.038	4.052
		APT	S-2		3.430		4.323	
	5 oz	S-1	3.537	3.765	4.470	4.519	4.789	4.847
		APT	S-2		3.993		4.568	
28 day	0 oz	S-1	3.181	3.255	4.594	4.659	4.429	4.441
		APT	S-2		3.330		4.724	
	3 oz	S-1	3.801	3.841	4.660	4.691	4.813	4.923
		APT	S-2		3.880		4.722	
	5 oz	S-1	4.043	3.982	4.834	4.882	5.206	5.345
		APT	S-2		3.922		4.930	

## 5.6 Shrinkage Test Results

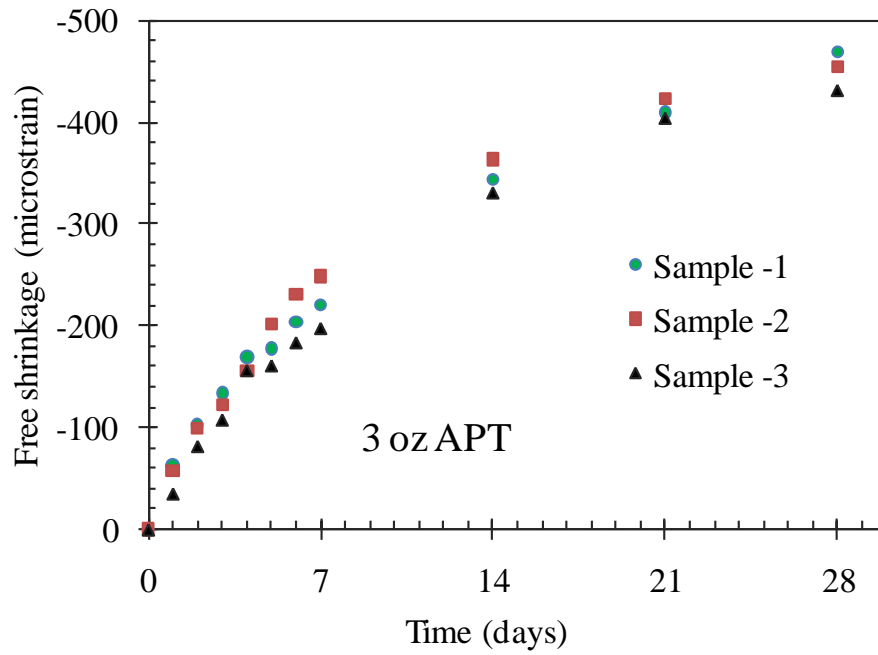
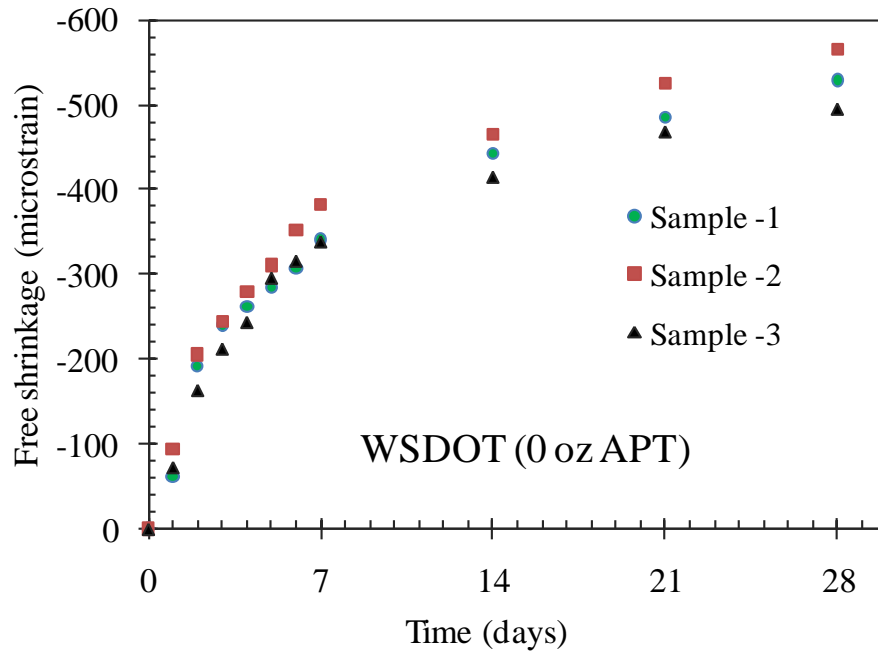
### 5.6.1 Free shrinkage test results

The free shrinkage test is performed according to AASHTO T 160 (ASTM C 157) “Length Change of Hardened Hydraulic Cement Mortar and Concrete”. Three prism concrete specimens for each group with dimensions of  $4 \times 4 \times 11.25$  in. ( $101.6 \times 101.6 \times 285.75$  mm) were cast. All the prisms were demolded at 24 hours after casting and then moved to the condition room for testing. The free shrinkage testing frame is shown in

**Figure 5.9.** Free shrinkage readings were recorded at every 24 hours for the first 7 days and then on the 14th, 21st, and 28th days, respectively. The free shrinkage test results are presented in **Figure 5.10** and **Table 5.4**.



**Figure 5.9 Free Shrinkage Test Setup.**



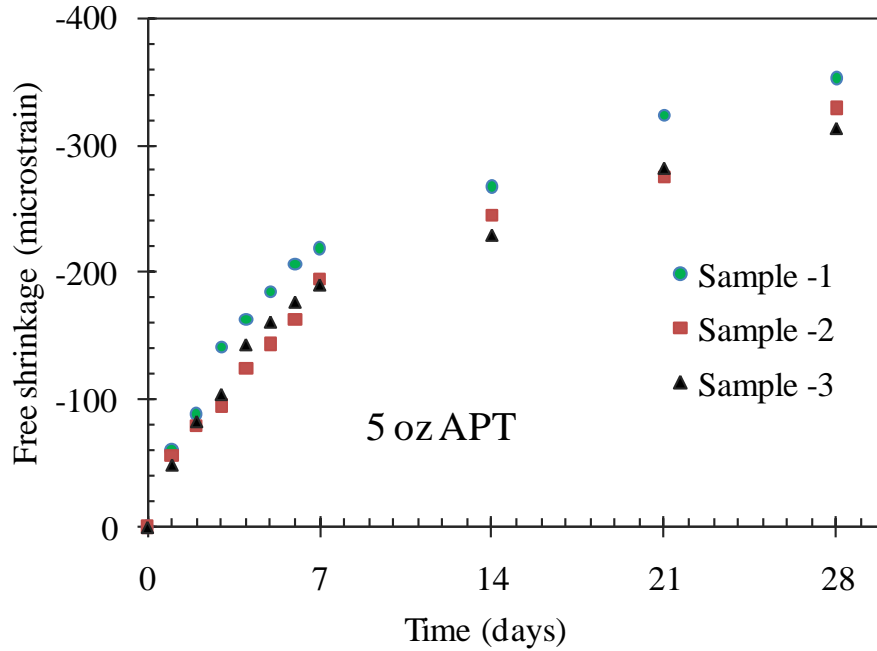


**Figure 5.10 Free Shrinkage of RAC with Different Amount of APT.**

**Table 5.4 Free Shrinkage Test Data (in microstrain)**

Days	WSDOT (0 oz APT)				3 oz APT				5 oz APT			
	S-1	S-2	S-3	Ave.	S-1	S-2	S-3	Ave.	S-1	S-2	S-3	Ave.
0	0.0	0.0	0.0	0.0	0.0	0.0	0.0	0.0	0.0	0.0	0.0	0.0
1	-61.3	-94.0	-72.7	-76.0	-62.5	-57.3	-35.3	-51.7	-60.4	-56.2	-49.1	-55.2
2	-191.3	-206.0	-163.3	-186.9	-102.7	-99.3	-82.0	-94.7	-88.9	-79.6	-83.2	-83.9
3	-240.7	-244.7	-212.0	-232.4	-134.0	-122.0	-108.0	-121.3	-141.5	-95.3	-104.5	-113.8
4	-262.0	-279.3	-243.3	-261.6	-169.3	-156.0	-156.7	-160.7	-162.8	-124.4	-143.6	-143.6
5	-284.0	-311.3	-295.3	-296.9	-177.3	-202.0	-161.3	-180.2	-184.2	-143.6	-161.4	-163.1
6	-308.0	-352.0	-315.3	-325.1	-204.0	-231.3	-184.0	-206.4	-206.9	-162.8	-177.1	-182.3
7	-340.7	-382.7	-338.0	-353.8	-220.7	-248.7	-198.0	-222.4	-219.0	-194.8	-190.6	-201.5
14	-443.3	-465.3	-414.0	-440.9	-344.0	-363.3	-331.3	-346.2	-267.7	-245.3	-229.7	-247.6
21	-484.7	-526.0	-467.3	-492.7	-409.3	-422.7	-404.7	-412.2	-323.6	-274.5	-282.3	-293.5
28	-529.3	-565.3	-494.0	-529.6	-468.7	-454.0	-432.0	-451.6	-352.7	-329.2	-313.6	-331.9

As we can see from **Figure 5.10** and **Table 5.4**, the free shrinkage of RAC without adding of APT is much larger than those with inclusion of APT. The reduced free shrinkage for RAC with 3 oz APT per gallon water at 7 and 28 days are 37.1% and 14.7%, respectively; while for RAC added with 5 oz APT per gallon water, the reduced free

shrinkage at 7 and 28 days are 43.1% and 37.3%, respectively. According to the WSDOT requirement, the maximum free shrinkage value of concrete with normal aggregate based on the WSDOT standard mix design should be less than 320 microstrain at 28-day. Therefore, the average free shrinkage of the studied RAC samples with inclusion of 5 oz. APT/gallon of water at 28 day is about 332 microstrain (see Table 5.4) which nearly meets the WSDOT shrinkage requirement.

### 5.6.2 Restrained shrinkage test results

As aforementioned, the ring test method is used to evaluate the relative drying shrinkage cracking tendency of RAC with different amount of APT. The ring test restrains the concrete using a steel ring, thus inducing a tensile stress on the surrounding concrete ring. When this stress becomes larger than the tensile strength of the concrete ring, the concrete ring will crack. The time that it takes for RAC ring samples with different amount of APT to crack are recorded and then compared with each other. The longer it takes a concrete ring specimen to crack, the lower tendency of drying shrinkage cracking it has. The time (days) that all the specimens took to crack are listed in **Table 5.5**, and the restrained ring test data for all specimens are shown in **Figure 5.11** to **Figure 5.13**. From those figures, it obviously shows that the time that it took for RAC ring samples to crack increased as the increase of the enclosed amount of APT in the mixture, demonstrating that the APT is an effective and efficient admixture to significantly reduce the drying shrinkage cracking of RAC.

**Table 5.5 Restrained Ring Test Data (days of cracking)**

Mixtures	Sample-1	Sample-2
WSDOT (0 oz APT)	17.1	18.9
3 oz APT	20.2	24.1
5 oz APT	23.7	No crack

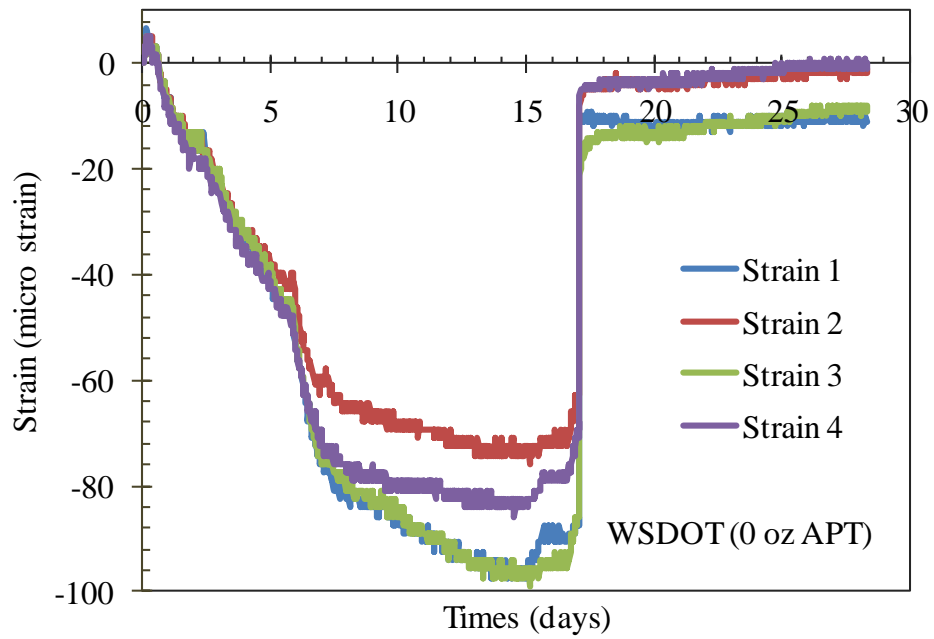
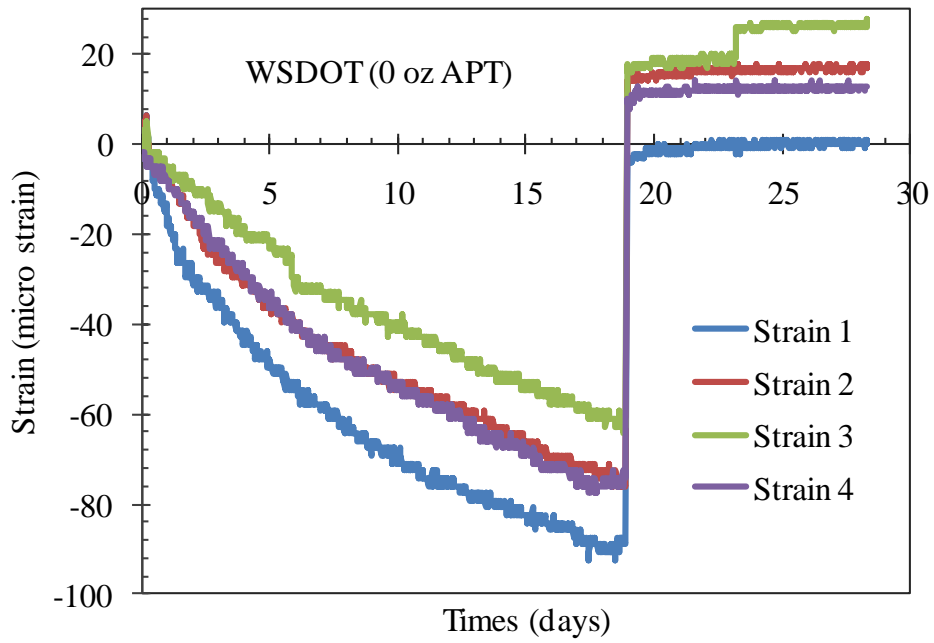


**Figure 5.11 Restrained Shrinkage of Ring Specimen without APT.**

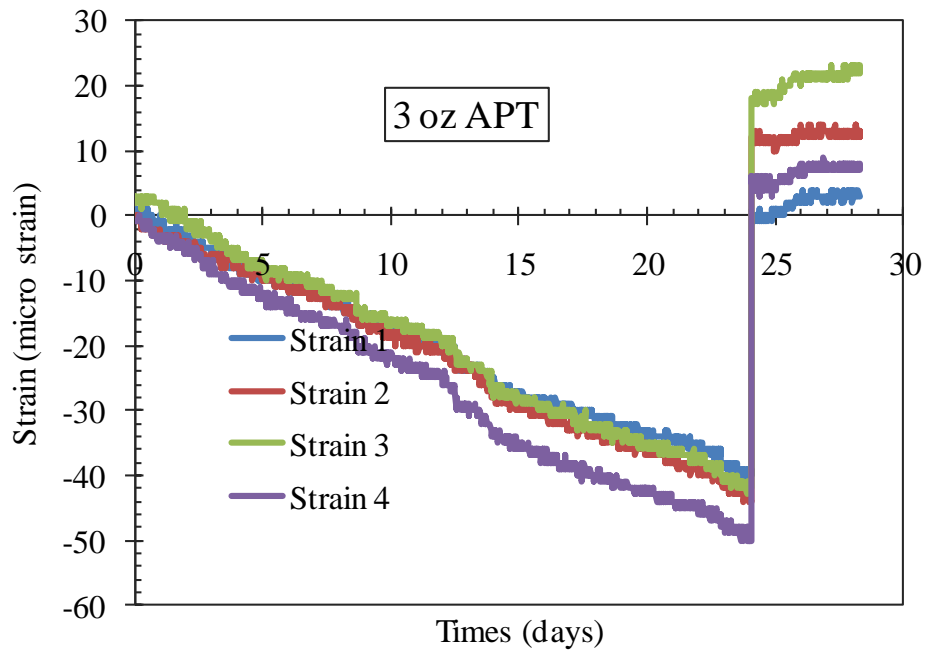
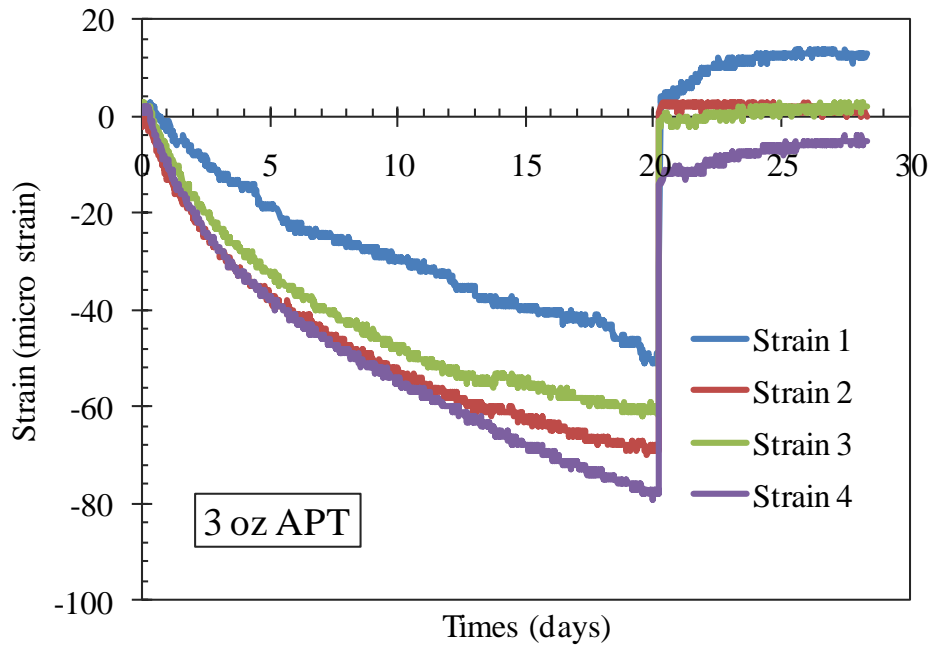


**Figure 5.12 Restrained Shrinkage of Ring Specimen with 3 oz APT/gallon of Water.**

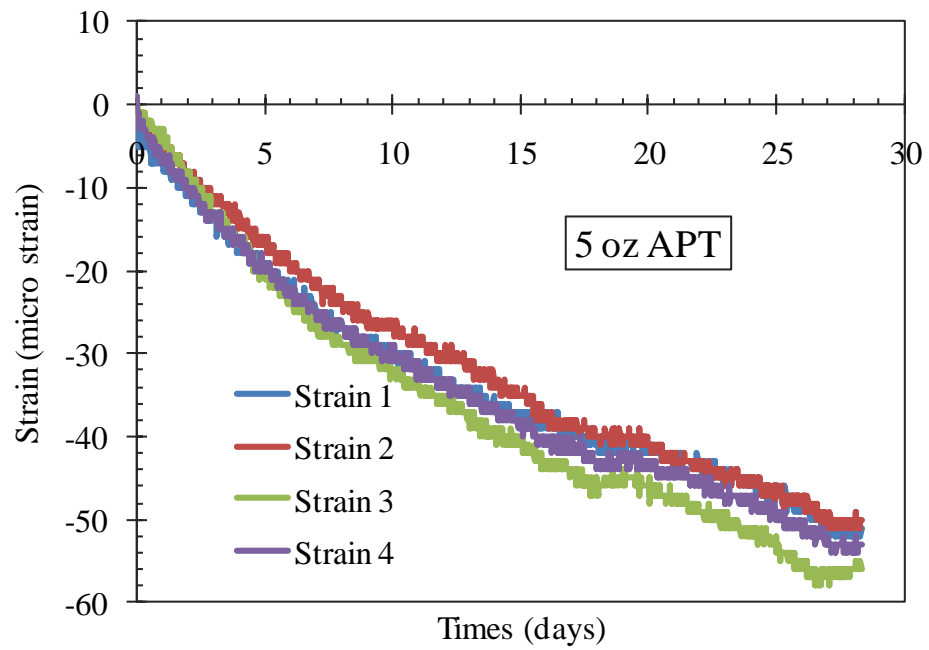
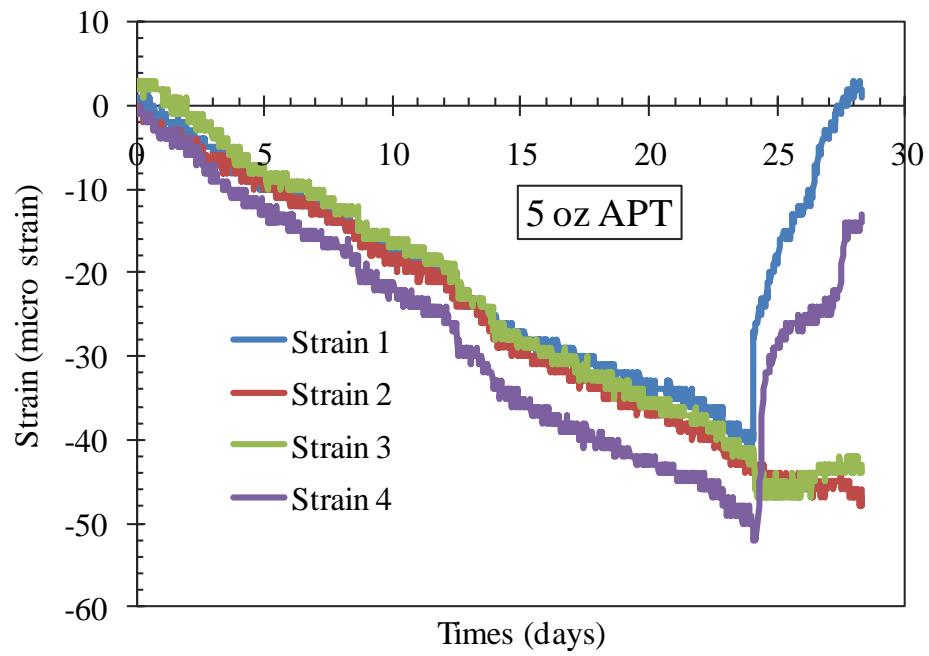


**Figure 5.13. Restrained Shrinkage of Ring Specimen with 5 oz APT/gallon of Water.**

## **Chapter 6 Conclusions and Recommendations**

The goal of this project is to characterize the enhancement effect of atomic polymer technology (APT) in form of mesoporous inorganic polymer (MIP) on material and durability properties of recycled aggregate concrete (RAC) and develop health monitoring techniques using smart aggregate. A comprehensive literature review on both RAC and smart piezoelectric sensors/actuators for health monitoring of concrete was first conducted. Based on the literature review, it is concluded that the mechanical and durability properties of RAC are usually lower than those of its counterpart of natural aggregate concrete (NAC), due to low density, high porosity, and high water absorption brought by the recycled aggregates (RA). The RAC samples added with different amount of APTs were prepared and measured, from which the basic material and durability properties, such as stiffness, strength and earlier shrinkage, were measured. The smart aggregates made of cement modules enclosing the PZT patches were fabricated, and they were embedded in concrete beams to monitor the earlier stiffness gaining process of the RAC samples during its curing stage. The corresponding monitoring technique based on the wave propagation was developed and implemented. It demonstrated that the APT admixture is able to effectively improve the material durability and performance of RAC and the proposed monitoring technique is capable of assessing and measuring the stiffness gaining process of RAC during its curing stage.

### **6.1 Conclusions**

Based on the experimental characterization of RAC samples and implementation of smart aggregates in health monitoring of RAC prisms conducted in this study, the following preliminary conclusions are obtained:

1. Based on the static compression test results, the Young's modulus, compressive and flexural strength of the RAC increase as the increase of the added APT, among which the compressive strength of RAC at 7 days increased as much as 42% by adding 5 oz APT/gallon of water, indicating that the APT is a qualified and promising admixture to effectively improve the material properties of RAC.
2. Based on the dynamic modulus test data, the frequency and dynamic modulus of the RAC samples gradually increase with the increase of the curing time, representing the stiffness and strength gaining process during its curing period. However, the frequency and dynamic modulus of the RAC do not increase as obviously with the increase of the added APT as these obtained from the compression test, indicating that the global dynamic modulus is not an appealing parameter to characterize the effect of the APT on the earlier stiffness of RAC.
3. The health monitoring technique using embedded smart aggregates show its capability of assessing and measuring the stiffness gaining process of RAC during its curing stage. Most importantly, the effect of the added APT on the earlier stiffness of RAC can be obviously observed based on the elastic wave test, as noticed by the significant increase of both the extension and shear modulus with respect to the increased inclusion of APT.
4. The comparison of the elastic modulus of the studied RAC samples based on different test methods (i.e., static compressive test, dynamic modulus test, and elastic wave-based test) shows that the static compressive test predicts the lowest value whereas the elastic wave-based test predicts the highest value of elastic modulus of RAC.
5. The free shrinkage of RAC without adding APT is much larger than those added with APT. The reduced free shrinkage for RAC added with 3 oz APT per gallon of water at 7 and 28 days are 37.1% and 14.7%, respectively; while for RAC

added with 5 oz APT per gallon of water, the reduced free shrinkage at 7 and 28 days are 43.1% and 37.3%, respectively. The free shrinkage of the studied RAC samples based on the WSDOT benchmark mix design will basically meet the WSDOT shrinkage requirement by adding 5 oz APT/gallon of water.

6. Based on the test results of relative drying shrinkage cracking tendency of RAC with different amount of APT, the time that it took for RAC ring samples to crack increase as the increase of the added APT, which demonstrates that the APT is an effective and efficient admixture to significantly reduce the drying shrinkage cracking of RAC.

## **6.2 Recommendations**

Based on the experimental program conducted and the health monitoring techniques developed in this study, the following recommendations are suggested for promoting application of recycled aggregate concrete (RAC) as well as the atomic polymer technology (APT) in transportation construction and providing viable and effective health monitoring techniques for concrete structures in general.

1. Though it is anticipated that the mechanical and durability properties of RAC are generally lower than those of NAC, RAC is recommended for the use in the transportation construction as long as their basic material properties meet the DOT's requirements by adding appropriate amount of APT admixture.
2. The long term performance of RAC should be monitored, using either the conventional dynamic modulus test (ASTM C215) or the proposed smart health monitoring technique with embedded smart aggregates which is capable of in situ assessing the condition of concrete materials.

3. The atomic polymer technology (APT) in form of mesoporous inorganic polymer (MIP) is highly recommended as an efficient admixture for RAC performance enhancement to meet both the free and drying shrinkage requirement.

### **ACKNOWLEDGEMENTS**

This research was supported by the Transportation Northwest (TransNow Regional Center)/USDOT. The recycled aggregates used in this study were donated by Central Pre-Mix Concrete Co. of Spokane, WA (Craig L. Matteson), and their generosity is gratefully acknowledged. The assistance provided by the graduate students Wei Fan, Nicolas Lopez, Huajie Wen, and visiting scholar Guobao Zhou in the experimental study is acknowledged.

## References

- AASHTO PP34-99 (2006) “Standard Practice for Estimating the Crack Tendency of Concrete,” *AASHTO Provisional Standards*, Washington D.C.
- Adom-Asamoah, M. and Afrifa, R. O. A study of concrete properties using phyllite as coarse aggregates. *Materials and Design*, 31(2010): 4561–4566.
- Ajdukiewicz, A. and Kliszczewicz, A. (2002). “Influence of recycled aggregates on mechanical properties of HS/HPC,” *Cement and Concrete Composites*, 24(2):69-79.
- ASTM C215, Test Method for Fundamental Transverse, Longitudinal, and Torsional Frequencies of Concrete Specimens, Annual Book of ASTM Standards, vol. 04.02, American Society for Testing and Materials, Philadelphia, 1992.
- ASTM C666, Standard Test Method for Resistance of Concrete to Rapid Freezing and Thawing, Annual Book of ASTM Standards, vol. 04.02, American Society for Testing and Materials, Philadelphia, 1992, 347-352.
- BCSJ (1978). “Study on recycled aggregate and recycled aggregate concrete,” Building Contractors Society of Japan, Committee on Disposal and Reuse of Concrete Construction Waste, *Summary in Concrete Journal*, Japan, 16(7): 18-31 (in Japanese).
- Brito, J., Pereira, A.S., and Correia, J.R. (2005). “Mechanical behavior of non-structural concrete made with recycled ceramic aggregates,” *Cement and Concrete Composites*, 27: 429-433.
- Buyle-Bodin, F. and Hadjieva-Zaharieva, R. (2002). “Influence of industrially produced recycled aggregates on flow properties of concrete,” *Materials and Structures*, 35(8): 504-509.
- Bloom, R. and Bentur, A. (1995) “Free and Restrained Shrinkage of Normal and High-strength Concretes,” *ACI Materials Journal*, Vol. 92, No. 2, Mar.-Apr., pp. 211-217.

- Darwin, D., Lindquist, W.D., McLeod, H. A. K., and Browning, J. (2007). "Mineral Admixtures, Curing, and Concrete Shrinkage", Ninth Canmet/ACI International Conference on Fly Ash, Silica Fume, Slag and Natural Pozzolans in Concrete, Warsaw, Poland.
- Debieb, F., Courard, L., and Kenai, S. Mechanical and durability properties of concrete using contaminated recycled aggregates. *Cement & Concrete Composites*, 32(2010):421–426.
- Delatte, N., Mack, E., and Cleary, J. (2007). "Evaluation of High Absorptive Materials to Improve Internal Curing of Low Permeability Concrete", State Job Number 134227, Final Report, Cleveland State University, Cleveland, OH.
- Domingo-Cabo, A., Lázaro, C., López-Gayarre, F., et al. (2009). "Creep and shrinkage of recycled aggregate concrete," *Construction and Building Materials*, 23(7): 2545-2553.
- Domingo, A., Lázaro, C., and Gayarre, F. L. Long term deformations by creep and shrinkage in recycled aggregate concrete. *Materials and Structures*, 43(2010):1147–1160
- Du, T., Wang W., and Liu, Z. The complete stress-strain curve of recycled aggregate concrete under uniaxial compression loading. *Journal of Wuhan University of Technology-Materials*, 25(2010):862-865.
- Fonseca, N., de Brito, J., and Evangelista, L. The influence of curing conditions on the mechanical performance of concrete made with recycled concrete waste. *Cement & Concrete Composites*, 33(2011):637–643.
- Frondistou-Yannas, S. (1977). "Waste concrete as aggregate for new concrete," *Journal Proceedings, JL74-37*, 74(8): 373-376.
- Frondistou-Yannas, S. (1977). "Waste concrete as aggregate for new concrete," *Journal Proceedings, JL74-37*, 74(8): 373-376.

- Gómez-Soberón, J. M. V. (2002). "Porosity of recycled concrete with substitution of recycled concrete aggregate: An experimental study," *Cement and Concrete Research*, 32(8): 1301-1311.
- Hansen, T.C. and Narud, H. (1983). "Strength of recycled concrete made from crushed concrete coarse aggregate," *Concrete International*, 5(1):79-83.
- Hasaba, S., et.al. (1981). "Drying shrinkage and durability of concrete made of recycled concrete," *Transition of the Japan Concrete Institute*, 3:55-60.
- Hansen, T.C. and Boegh, E. (1985). "Elasticity and drying shrinkage of recycled aggregate concrete," *ACI Journal*, Sep-Oct, pp.648-652.
- Hiroshi, T, Atsushi, N., et al. (2001). "High quality recycled aggregate concrete (HiRCA) processed by decompression and rapid release," *ACI Special Publications*, Rep. No. SP-200, American Concrete Institute (ACI), Detroit, pp. 491–502.
- Katz, A. (2003). "Properties of concrete made with recycled aggregate from partially hydrated old concrete," *Cement and Concrete Research*, 33: 703-711.
- Kelly, T. (1998). "Crushed cement concrete substitution for construction aggregates-a materials flow analysis," *U.S. Geological Survey Circular 1177*, pp. 2.
- Kou, Shi-cong, Poon, Chi-sun and Agrela, F. Comparisons of natural and recycled aggregate concretes prepared with the addition of different mineral admixtures. *Cement & Concrete Composites*, 33(2011):788–795
- Kou, Shi-cong and Poon, Chi-sun. Properties of concrete prepared with PVA-impregnated recycled concrete aggregates. *Cement & Concrete Composites*, 32(2010):649–654.
- Krauss, P.D. and Rogalla, E.A. (1996). "Transverse Cracking in Newly Constructed Bridge Decks", National Cooperative Highway Research Program (NCHRP) Report 380, Transportation Research Board.
- Kreijger, P.C. et al. (1987). "Ecological properties of building materials," *Materials and Structures*, 20(4): 248-254.

- Levy, S.M. and Helene, P. (2004). “Durability of recycled aggregates concrete: a safe way to sustainable development,” *Cement and Concrete Research*, 34:1975–1980
- Limbachiya, M. C., Leelawat, T. and Dhir, R.K. (2000). “Use of recycled concrete aggregate in high-strength concrete,” *Materials and Structures*, 33(9): 574-580.
- Liu, Q., Xiao, J., and Sun, Z. Experimental study on the failure mechanism of recycled concrete. *Cement and Concrete Research*, 41(2011):1050–1057.
- Hansen, T.C. and Boegh, E. (1985). “Elasticity and drying shrinkage of recycled aggregate concrete,” *ACI Journal*, Sep-Oct, pp.648-652.
- Mindess, S., Young, J.F. and Darwin, D. (2003). “*Concrete*”, 2nd edition, Prentice-Hall, Upper Saddle River, N.J., 644 pp.
- Nataraja, N.C and Das, L. A simplified mix proportioning for cement based composites with crushed tile waste aggregate. *Journal of Scientific & Industrial Research*, 70(2011):385-390.
- Nilsen, A.U. and Monteiro, P.J.M. (1993). “Concrete: A three phase material,” *Cement and Concrete Research*, 23(1):147-151.
- Nixon, P. J. (1978). “Recycled concrete as an aggregate for concrete - A review,” *Materials and Structures*, 11(6), 371-378.
- Oikonomou, N.D. (2005). “Recycled concrete aggregates,” *Cement and Concrete Composites*, 27: 315–318.
- Paillère, A. M., Buil, M., and Serrano, J. J. (1989) “Effect of Fiber Addition on the Autogenous Shrinkage of Silica Fume Concrete”, *ACI Materials Journal*, Vol. 86, No. 2, Mar.-Apr., pp. 139-144.
- Rao, M.C., Bhattacharyya, S. K., and Barai, S. V. Influence of field recycled coarse aggregate on properties of concrete. *Materials and Structures*, 44(2011):205–220
- Ravindrarajah, S. and Tam, R. (1985). “Properties of concrete made with crushed concrete as coarse aggregate,” *Magazine of Concrete Research*, 37(130): 29-38.

- Ridzuan, A.R.M. et al. (2001). "The influence of recycled aggregate concrete on early compressive strength and drying shrinkage of concrete," *Proceeding of the International Conference on Structural Engineering, Mechanics and Computation*, Cape Town, South Africa, pp.1415-1421.
- Rogoff, M.J. and Williams, J.F. (1994). *Approaches to Implementing Solid Waste Recycling Facilities*. Noyes Publications
- Ryu, J.S. (2002). "Improvement on strength and impermeability of recycled concrete made from crushed concrete coarse aggregate," *Journal of Material Science Letters*, 21:1565-1567.
- Salem, R. M. (1996). *Strength and Durability Characteristics of Recycled Aggregate Concrete*. PhD Dissertation, University of Tennessee, Knoxville, TN.
- Salem, R.M., Burdette, E.G., and Jackson, N.M. (2003). "Resistance to freezing and thawing of recycled aggregate concrete," *ACI Materials Journal*, May-June, pp.216-221.
- Schaels, C. A., and K. C. Hover. (1988) "Influence of Mix Proportions and Construction Operations on Plastic Shrinkage Cracking in Thin Slabs", *ACI Materials Journal*, Vol. 85, pp. 495-504.
- Song, G., Mo, Y.L., Otero, K., et al. (2006). "Health monitoring and rehabilitation of a concrete structure using intelligent materials," *Smart Materials and Structures*, 15(2): 309-314.
- Song, G.B., Gu, H.C., and Mo, Y.L. (2008). "Smart aggregates: multi-functional sensors for concrete structures - a tutorial and a review," *Smart Materials and Structures*, 17(3).
- Sun, M.Q., Staszewski, W.J., Swamy, R.N., et al. (2008). "Application of low-profile piezoceramic transducers for health monitoring of concrete structures," *NDT & E International*, 41(8):589-595.

- Tavakoli, M. and Soroushian, P. (1996). "Strengths of recycled aggregate concrete made using field-demolished concrete as aggregate," *ACI Materials Journal*, 93(2):178-181.
- Topcu, I.B. and Sengel, S. (2004). "Properties of concretes produced with waste concrete aggregate," *Cement and Concrete Research*, 34: 1307–1312.
- Tritsch, N., Darwin, D. and Browning J. (2005). "Evaluating Shrinkage and Cracking Behavior of Concrete Using Restrained Ring and Free Shrinkage Tests", The Transportation Pooled Fund Program Project No. TPF-5(051), Structural Engineering and Engineering Materials SM Report No.77, The University of Kansas Center for Research, Inc. at Kansas
- Wu, F. and Chang, F.-K. (2006a). "Debond detection using embedded piezoelectric elements in reinforced concrete structures – Part I: Experiment," *Structure Health Monitoring*, 5:5-15.
- Wu, F. and Chang, F.-K. (2006b). "Debond detection using embedded piezoelectric elements for reinforced concrete structures – Part II: Analysis and algorithm," *Structure Health Monitoring*, 5:17-28.
- Xiao, J.Z., Li, J.B., and Zhang, C. (2005). "Mechanical properties of recycled aggregate concrete under uniaxial loading," *Cement and Concrete Research*, 35:1187-1194.
- Yan, S., Sun, W., Song, G.B., et al. (2009). "Health monitoring of reinforced concrete shear walls using smart aggregates," *Smart Materials and Structures*, 18(4).
- Yoda, K. and Yoshikane, T. (1988). "Recycled cement and recycled in Japan," *Proceedings of Second International RILEM Symposium on Demolition and Ruse of Concrete and Masonry*, Tokyo, Japan, pp.527-536.
- Zaharieva, R., Buyle-Bodin, F. and Wirquin, E. (2004). "Frost resistance of recycled aggregate concrete," *Cement and Concrete Research*, 34:1927-1932.